Report No. FHWA-RD-79-48

EVALUATION OF HORIZONTAL CURVE DESIGN

August 1980
Final Report

Document is available to the public through the National Technical Information Service, Springfield, Virginia 22161

Prepared for
FEDERAL HIGHWAY ADMINISTRATION
Offices of Research & Development
Environmental Division
Washington, D.C. 20590

FOREWORD

This report documents results from a program of research in which observational and analytical evaluations of horizontal curve design criteria were made. Observational data were collected for three categories of vehicles traversing three separate horizontal curves in order to obtain actual path and speed information. Analyses of both transient and steady-state dynamics of three categories of vehicles traversing idealized curves were made with the use of the Highway-Vehicle-Object Simulation Model (HVOSM). The report will be of interest to traffic and highway design engineers concerned with highway geometrics and the effects of geometrics on traffic operations.

This research program was conducted by the Advanced Technology Center of Calspan Corporation for the U.S. Department of Transportation, Federal Highway Administration, as part of the Federally Coordinated Program (FCP) of Research and Development. The Federal Highway Administration project manager was Mr. George B. Pilkington, II.

The authors would like to acknowledge the efforts of Mr. Timothy S. Johnson, whose aid in collection of the observational data was invaluable, and the efforts of Ms. Maureen E. Ball and Ms. Janice E. Mulartrick for preparation of the manuscript.

A selective distribution is being made by the sponsoring FHWA division. A limited number of copies of this report are available for official use from the Federal Highway Administration, Environmental Division, HRS-43, Washington, D.C. 20590. This document is also available to the public through the National Technical Information Service (NTIS), Springfield, Virginia 22161. A fee will be charged for all copies ordered through NTIS.

Charles F. Scheffey
Director, Office of Research
Federal Highway Administration

NOTICE

Technical Report Documentation Page

1. Report No.	2. Government Accession No.	3. Recipient's Catalog No.
FHWA-RD-79-48		

4. Title and Subtitle	5. Report Date
EVALUATION OF HORIZONTAL CURVE DESIGN	August 1980
	6. Performing Organization Code
	8. Performing Organization Report No.
7. Author(s)	
David J. Segal and Thomas A. Banney	6188-V-1
9. Performing Organization Name and Address	10. Work Unit No. (TRAIS)
Calspan Corporation Advanced Technology Center P.O. Box 400 Buffalo, New York 14225	FCP 31J1092
	11. Contract or Grant No. DOT-FH-11-8501 (Mod. #7)
	13. Type of Report and Period Covered
12. Sponsoring Agency Name and Address	
U. S. Department of Transportation Federal Highway Administration Environmental Division Washington, D.C. 20590	Final Report
	14. Sponsoring Agency Code

15. Supplementary Notes

FHWA Project Manager: George B. Pilkington, II (HRS-43)

16. Abstract

This report documents an initial evaluation of horizontal curve design criteria which involved two phases: an observational study and an analytical evaluation. Three classes of vehicles (automobiles, school buses and tractor semi-trailers) and three selected curves (8, 31 and 38) were utilized in the study in order to determine vehicle path and speed. The analytical evaluation using the HVOSM was conducted to relate the vehicle dynamics during curve traversal to horizontal curve design criteria. Horizontal curve parameters were curve radius, vehicle class, speed, curve transition type and super-elevation rate. The report suggests that the use of spiral transition curves in horizontal alignment would improve traffic operations and recommends further research to confirm the change in steady-state steer characteristics on superelevated curves.

17. Key Words	18. Distribution Statement
Highway Design, Horizontal Curve Design, Driver Behavior, Vehicle Dynamics, HVOSM	No restrictions. This document is available to the public through the National Technical Information Service, Springfield, Virginia 22161

19. Security Classif. (of this report)	20. Security Classif. (of this page)	21. No. of Pages	22. Price
Unclassified	Unclassified	106	

TABLE OF CONTENTS

LIST OF FIGURES

LIST OF FIGURES (Continued)

LIST OF TABLES

1. INTRODUCTION

The objective of the work reported herein has been to provide an initial evaluation of the applicability of existing horizontal curve design criteria to real world operating conditions. The geometric design of horizontal curves for highways has historically been based on empiricism and point-mass, steady-state kinematic theory. Effects that this design philosophy have had on the transient and steady-state dynamics of the widely varying types and sizes of vehicles using the highway system have been largely unexplored. Conversely, the role, if any, that vehicle dynamics should have in establishing horizontal curve design criteria has not been established.

While it must be recognized that existing highway curves are successfully negotiated by the vast majority of vehicles traversing them, very little is known about how drivers actually guide their vehicles around the curve or the extent of the burden that the curve imposes on the driver. Recent, widely publicized accidents involving loss-of-control on curves have prompted this study with the intent of identifying whether any aspect of existing design criteria may contribute to the difficulties that various classes of vehicles experience in negotiating curves.

This study was organized into three tasks. The first task involved a search of the literature to determine which vehicle simulation models were applicable for use in a subsequent task. This effort concentrated on finding an articulated vehicle simulation model that contained provisions for automatic guidance and non-uniform terrain. The second task was undertaken in order to determine how various vehicle classes negotiate curves. This task involved the unobtrusive observation of automobiles, school buses and articulated vehicles (tractor/semi-trailers) traversing three different horizontal curves for the purpose of acquiring information to establish the paths used by the driver/vehicle combination and the speeds at which the curves were negotiated. The third task involved computer simulation of different vehicles traversing idealized curves. In this task the Highway-Vehicle-Object Simulation Model

(HVOSM), described in Reference 1, was used to study the transient and steady-state dynamics of three vehicles on curves of different radius, transition and superelevation rate.

A description of the methodology employed in both the observation and simulation of vehicles traversing curves is contained in Section 2 of this report. The results obtained in both the field observation and simulation tasks are presented and discussed in Section 3. Conclusions and Recommendations resulting from the study are contained in Section 4.

2. METHODOLOGY

The study reported herein consisted of two basic efforts to aid in the evaluation of existing design criteria for horizontal curves. Computer simulation techniques were employed to evaluate the effects of different curve design elements - degree of curve, superelevation and transition type - on the performance of various vehicle classes. In addition, observations and measurements of vehicles traversing three selected curves were made to aid in evaluating the results obtained from the computer simulation study. This effort was judged to be necessary due to the inherent limitiations of the computer simulation used - in particular the limitations of the automatic guidance (driver) algorithm to accurately predict driver behavior. The object was to provide an experimental data base by which the idealized results from the simulation could be extrapolated to real world situations. While a methodology for making this extrapolation was not successfully developed during this effort, it must be noted that both the simulation and observational tasks produced results that are valuable - the simulation results are valid for making relative comparisons between curve designs and the observational results provide a start at understanding the relationships between curve design and driver/vehicle behavior. The general methodology employed in performing these two tasks is described in the two subsequent sections. Additional detail is given in Appendices A, B and C.

2.1 Collection of Observational Data

Constraints on the simulation task required study of 10°, 30° and 36° curves. It was therefore necessary to select observational sites with about the same degrees-of-curvature. However, additional criteria were also employed in the selection process based on practical considerations of traffic volume, mix and flow, as well as geometrical considerations such as approach to the curve and grade throughout.

Curves that met these criteria were located on entrance/exit ramps on limited access highways in the Buffalo area. The curves which best met all of the criteria were approximately 8°, 31° and 38°. A detailed description of each of the curves is given in Appendix A.

Data collected at each of the sites included vehicle velocity and right rear wheel offset from the road edge for the three vehicle classes - passenger car, schoolbus and tractor-trailer - observed. To collect this data, the curve sites were broken into three major intervals, over which an average speed was derived from a measured traversal time and the known distance. These major intervals were further divided into five evenly spaced sub-intervals. Wheel offsets were obtained at these positions.

The data collection procedure employed a chase car containing a driver and passenger. This car was stationed upstream from the curve and merged with and followed the subject vehicles throughout the curve. The driver operated timing equipment at appropriate points along the curve from which speeds were derived, while the passenger photographed the subject vehicle with a battery-operated motor drive 35 mm SLR camera. Subsequently, measurements of projections of these photographic negatives provided lateral position of the subject vehicle's right rear wheel throughout the curve.

For each of the selected curves, data were collected for three specified vehicle types:

1) passenger cars
2) full size school buses
3) tractor-trailers.

It was originally intended to collect 30 of each vehicle type on each curve, or 270 vehicle paths. Because of time constraints and the relative infrequency of school bus traffic (and tractor-trailer traffic on the 8° curve), smaller samples were obtained. Sample size was also reduced due to the disqualification of certain vehicles as not being in a free flow condition. Film quality, including difficulty of obtaining required measurements was also responsible for the reduction of usable sample size. Where data for more than 30 vehicles were collected, the sample was reduced to 30 vehicles based upon the quality of the data. The following table presents the sample sizes for each of the curves in terms of vehicle type (Table 1).

Table 1.

OBSERVATIONAL SAMPLE

Vehicle Type	38° Curve	8° Curve	31° Curve
Automobile	30	30	30
School Bus	30	13	14
Tractor-Trailer	30	20	30
TOTAL	90	63	74

2.2 Dynamic Evaluation of Horizontal Curves

Geometric design of horizontal curves has historically been based on empiricism and acceptance of steady-state kinematic theory. The influence that existing design criteria have on the dynamics of vehicles as they traverse curves, or inversely, the role that vehicle dynamics should have in influencing horizontal curve design criteria, are largely unknown. In order to obtain an initial understanding of the subtle inter-relationships that exist between the vehicle and the highway in this context, a detailed analytical tool providing the necessary generality in vehicle and roadway representation was required.

The Highway-Vehicle-Object Simulation Model (HVOSM) was therefore used in this study since it provided the necessary degree of generality, particularly with regard to its ability to accept varying terrain associated with superelevated curves. However, it should be noted that in its current form, the HVOSM does not provide the desirable capability for simulating articulated vehicles. This problem is further discussed in Section 3.2.

In addition to the basic HVOSM, a number of other requirements were needed to successfully accomplish the simulation study of horizontal curve design. These included:

- Minor modifications to the HVOSM to provide the capability of simulating dual wheel rear axles such as are common on school buses.

- Provision for automatically guiding the simulated vehicles along the prescribed paths which defined the curves of interest.

- Specification of the vehicles and the curves to be employed in the study.

These various items are further discussed below.

HVOSM Modifications

As the HVOSM, in its previous form, was able to directly model only four tires on a vehicle, minor modifications were required to the tire radial and side force calculations so that single tire data could be input and subsequently used to simulate dual rear tires. This modification, in a general sense, computes the side force of a single tire of the dual set based on one-half of the normal load on the axle side of interest and doubles this value to reflect the side force output of both tires. A more detailed description of the computational procedure is given in Appendix B.

This method of simulating dual tires allows input of individual tire parameters but calculates the total side force based on the assumptions that:

1. The radial force and tractive force for a set of duals is equally split between the two tires.
2. The slip angle is identical for each tire of the dual set.
3. The resultant forces acting on each of a set of dual tires can be replaced by a single set of forces acting at a location such that moment compatibility is maintained.

Automatic Guidance

A previously developed automatic guidance algorithm was initially used in the HVOSM in order to negotiate the simulated vehicles around the curves. This algorithm (Reference 3) allows input of a specified point attached to the vehicle sprung mass at which an error from a specified path is calculated. The error is then multiplied by a simple gain to produce a command steer angle to the front wheels.

The algorithm requires that the path which the vehicle is to follow be input as a series of coordinate pairs in the ground plane. These pairs are

then used to develop a continuous curve with piecewise cubic functions between pairs by a minimum energy spline fit technique.

For each of the vehicles simulated, a "wagon tongue" equivalent guidance system was modeled. The point at which error determinations were made was arbitrarily chosen to be one wheelbase ahead of the front wheels and a corresponding steering gain of 1/(wheelbase) radians/inch was applied to the system.

It should be pointed out that the results of this study, in terms of steering response, are a function of the vehicle, the curve, and the guidance system. Thus it cannot be expected that the responses of different vehicles to a given curve would be the same.

As the simulation task was about to be initiated, a checkout run of a compact car negotiating a 36° curve with a 90 ft. (27.4 m) spiral transition was examined in detail. The results of the command steer angle for this run are shown in Figure 1. After studying this run, it was determined that the high frequency content of the steer angle resulted from waviness of the piecewise cubic spline representation of the path. That is, while the spline fit passed through each of the x, y coordinate pairs, it varied from the ideal path between these pairs.

It was evident that this path representation would not be adequate for discrimination of the expected minor steer angle variations on which the curve design was to be studied. Thus, substantial modifications were made to the path following algorithm in an attempt to eliminate this problem. The path following algorithm was rewritten so that the path of each segment of the curve was determined implicitly. This was accomplished by breaking the individual curves into segments of tangent, spiral and constant radius paths. Errors associated with tangent and constant radius segments were determined from closed-form exact solutions to the geometrical problem knowing the position and orientation of the tangent, the center and radius of the circular segments and the position of the guide point fixed to the vehicle.

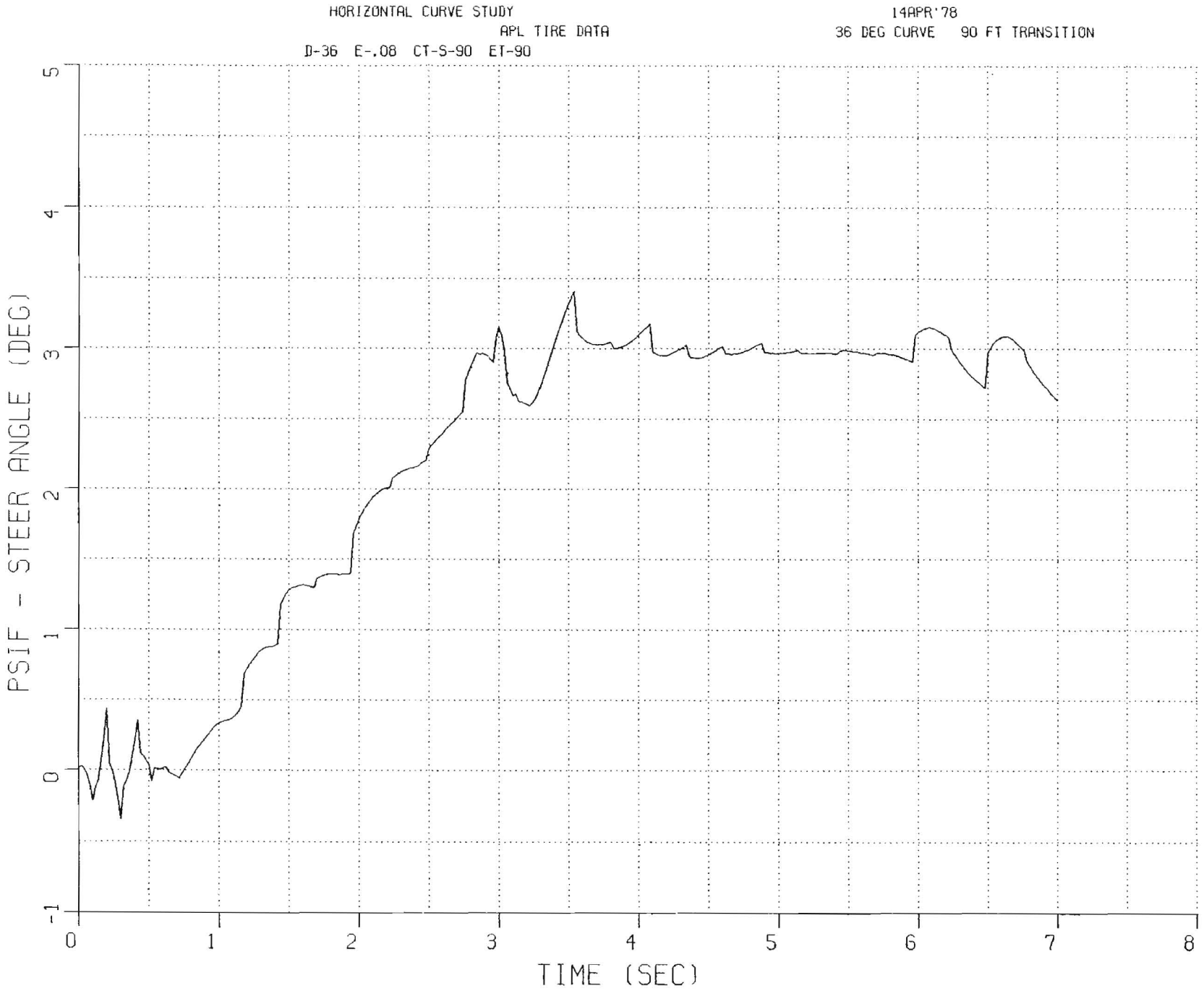

Figure 1. STEER ANGLE FROM INITIAL GUIDANCE ALGORITHM

Closed form solution to the steer error along a spiral segment could not be achieved. As indicated in Appendix D, solution of the position of a point on the spiral requires an integration of a function of the tangent angle of the spiral curve over the arc length. Thus, in order to determine a steering error, an iterative procedure was employed to find a point on the spiral that was located along a line passing through the vehicle guidance point and normal to the vehicle x-axis.

The result of this modification to the guidance algorithm is shown in Figure 2. Note that near the transition from tangent to spiral at about 0.5 seconds, high frequency content and minor discontinuities still result due to limitations on the accuracy with which the very small path errors that exist in that range could be determined. The steer angle increase along the spiral is well behaved; however, the response at about 2.9 seconds indicates that a discontinuity exists at the transition between the spiral and circular curve.

Detailed examination of this problem led to the explanation illustrated in Figure 3. As indicated on that figure, the tangent angle of the spiral at the junction between the spiral and circle is 61.2549°, and the tangent angle of the circle is 60.8984°. This 0.3565° discontinuity results in the sudden decrease in steer angle between 2.9 and 3.0 seconds on Figure 2. The cause of this angular difference stems from differences in the precision with which the spiral is generated within the HVOSM and within the pre-processing routine initially used to determine the curve path. The pre-processing routine used to develop the curve path and superelevation generated a spiral segment with a tangent angle at its end such that the center of curvature was located at the origin of the space fixed axis system. Consequently, the center of the circular portion of the curve was also located at the origin.

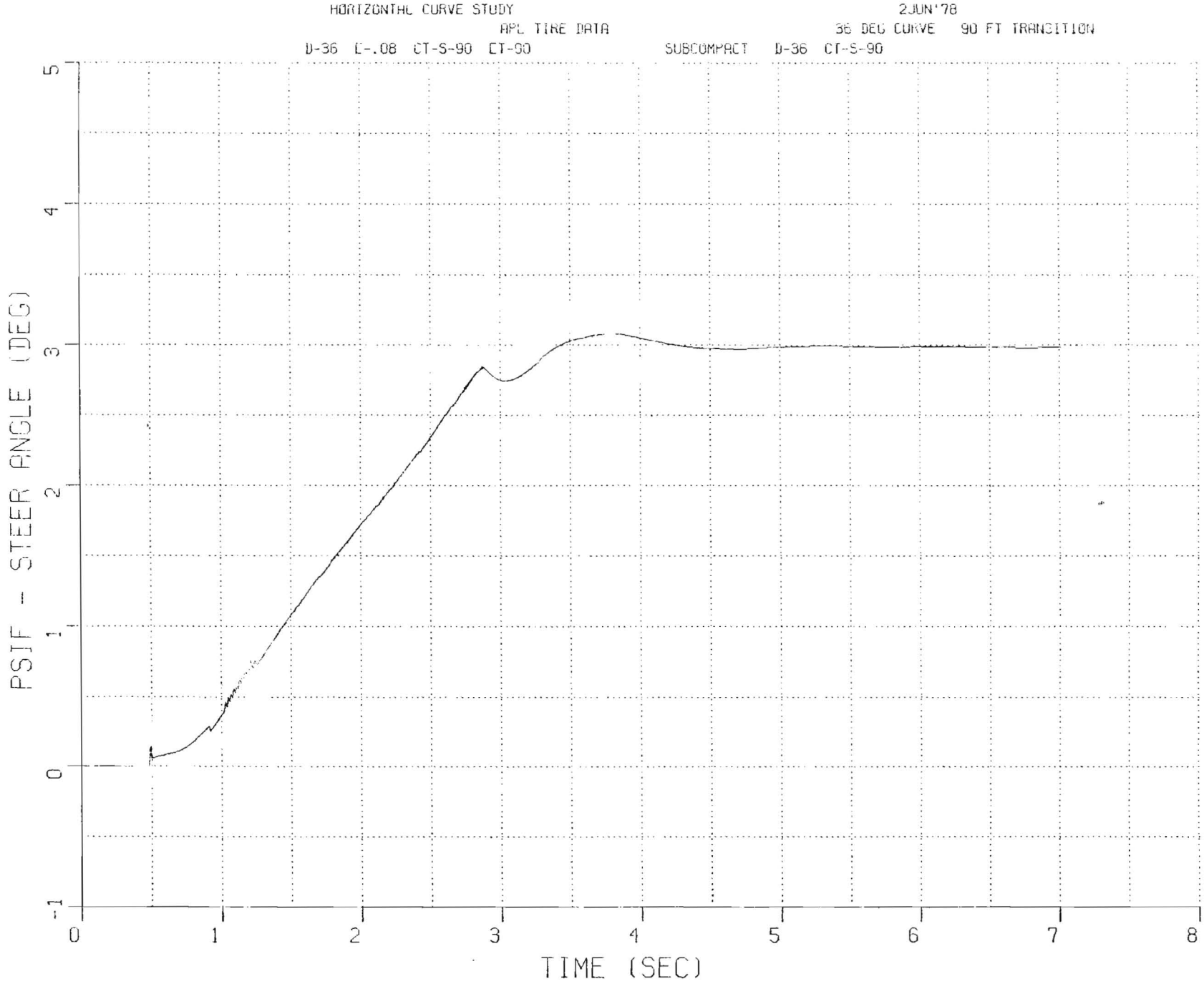

Figure 2. STEER ANGLE FROM MODIFIED GUIDANCE ALGORITHM

Figure 3. PATH DISCONTINUITY

In generating the same spiral segment within the modified automatic guidance algorithm of the HVOSM, differences in precision of computation resulted in the 0.3565° difference in tangent angle at the end of the spiral and a subsequent change in the center of curvature from the origin to a point located at x = -5.294 in. (134.47 mm) and y = 9.577 in. (243.26 mm). In order to eliminate this path discontinuity, it was necessary to then relocate the center of the circular curve segment to coincide with this point.

One potential problem inherent in this solution to the path discontinuity was that the terrain table representation of superelevation had been previously developed assuming that the ideal path would remain at zero elevation (i.e., the roadway rotated about the ideal path) and the center of the circular segment of the ideal path was at the space-fixed region. In moving this center off the origin, a path was obtained that no longer remained at zero elevation. Thus, an incompatibility in the modified path and terrain data resulted in the path either increasing or decreasing in elevation along its length.

As a check to insure that this artificially introduced gradient would not significantly influence the vehicle dynamics, a worst case evaluation of the gradient was made. For the 10 degree curve of radius 573 feet (174.6 m) the center of the circular portion of the curve moved off the origin by somewhat less than 2 feet. The attendant maximum change in path elevation (assuming .12 superelevation rate) was about 2 x .12 = .24 feet (73.2 mm). The average gradient along this circular arc between the start of the arc and the maximum elevation change is then approximately -3.3×10^{-3} inches/foot (-275×10^{-3} mm/m). This gradient was judged to have a negligible effect on the results and was therefore ignored.

Simulated Vehicles

Three categories of vehicles are employed in the simulation study of horizontal curve design requirements: a compact automobile; a full-size automobile; and a conventional 66 passenger school bus. Summaries of the input parameters required to describe these vehicles in the HVOSM are provided in Appendix C. The data describing the compact automobile was obtained from Mr. Paul Bohn of the Applied Physics Laboratory of Johns Hopkins University. Descriptive parameters for the full-size vehicle were obtained from Reference 4. No complete, directly applicable data set was available for describing a conventional 66 passenger school bus, so measurements of certain dimensional properties made by Calspan personnel together with information extracted from References 5, 6 and 7 formed the basis for estimated parameters for this vehicle. Note that while References 6 and 7 contained moment-of-inertia data for buses, they apply to inter-city rather than school buses. However these data were scaled based on dimensional and weight differences to provide moment-of-inertia estimates for the simulated school bus. Input data for simulating the 10.0 x 20.0 tires on the bus were obtained from measurements previously made by the Calspan Tire Research Facility.

Simulated Curves

Three basic curves of 36, 30 and 10 degrees were used for the simulation study of hypothetical curves. To each of these basic curves were applied three types of curve transition: spiral, compound curve and none. Furthermore, each curve was assumed to have superelevation of 8% and 12%.

The design speed for each of these curves was taken from Figure VII-8 on page 326 of A Policy on Geometric Design of Rural Highways* (Reference 8) based on the design speed criteria given for open highway curves.

*Hereafter referred to as the AASHTO Blue Book.

These approximate speeds for each basic curve are as follows:

Degree of Curve	Design Speed mph	(km/h)
36	26	(41.8)
30	28	(45.1)
10	46	(74.0)

Characteristics of the spiral transition for each of these curves were then obtained from Table VII-4 on page 327 of the AASTHO Blue Book for speeds near the established design speeds. These characteristics, the minimum length of the spiral and the assumed value of the rate of change of lateral acceleration (C), are:

Design Speed mph	(km/h)	Minimum Spiral Length ft	(m)	C ft/sec^3	(m/sec^3)
25	(40.2)	90	(27.4)	3.75	(1.14)
30	(48.3)	110	(33.5)	3.5	(1.07)
45	(72.4)	200	(61.0)	2.75	(0.84)

The development of the spiral transition* is based on the assumption of a constant rate-of-change of lateral acceleration and at a constant speed and, therefore a constant rate of change of curvature. This general form of this relationship is

$$k = \frac{C}{v^3} s$$

where k is the curvature, v is the velocity and s is the length along the spiral. With manipulation this relationship becomes the Shortt formula (page 174 of the AASHTO Blue Book):

$$L = \frac{AV^3}{RC}$$

*See Appendix D.

where L = length of spiral, ft (m)

V = speed, mph (km/h)

R = curve radius, ft (m)

C = rate of increase of centripetal acceleration, ft/sec^3 (m/sec^3)

A = constant for conversion of units

$= 3.15\ (ft/sec)^3/(mph)^3$

$= 0.0214\ (m/sec)^3/(km/h)^3$.

Using this relationship, together with the spiral length, curvature (or radius) at the end of the spiral, and rate of change of lateral acceleration given above, the velocities required to achieve the rates of change of lateral acceleration were determined and are given below.

Degree of Curve	Radius (ft)	(m)	Spiral Length ft	(m)	C ft/sec^3	m/sec^3	Speed mph	(km/h)
36°	159.15	(48.51)	90	(27.4)	3.75	(1.14)	25.73	(41.40)
30°	190.99	(58.21)	110	(33.5)	3.5	(1.07)	28.56	(45.95)
10°	572.96	(174.64)	200	(61.0)	2.75	(0.84)	46.40	(74.66)

These speeds were used as the nominal, or design speeds, in the simulation study and agree closely with the design speeds from Table VII-4 of the AASHTO Blue Book indicating consistency in recommended speeds and spiral characteristics.

Compound curve transitions were developed based on the recommendation given in Table VII-5 on page 329 and Figure VII-9 on page 330 of the AASHTO Blue Book. The three-centered compound curves resulting from these recommendations are summarized below.

	Radius		Arc Length	
	ft	(m)	ft	(m)
36° Curve	159.15	(48.51)	-	-
2nd Circular Arc	320	(97.54)	70	(21.34)
1st Circular Arc	640	(195.07)	140	(42.67)
36° Curve	190.99	(58.21)	-	-
2nd Circular Arc	380	(115.83)	90	(27.43)
1st Circular Arc	760	(231.65)	180	(54.86)
10° Curve	572.96	(174.64)	-	-
2nd Circular Arc	1140	(347.48)	200	(60.96)
1st Circular Arc	2280	(694.95)	200	(60.96)

For each of the basic curves, superelevation rates of 8 and 12% were assumed to exist on the circular curve. Transitions in superelevation were therefore necessary from the flat tangent section to the superelevated curve. The superelevation transition for the spiral curve transitions were assumed to take place linearly with arc length along the spiral. For the compound curve transitions, superelevation varied linearly along the arc length for the two transition arcs before reaching its maximum at the start of the curve section.

For the case of tangent section to circular curve with no transition, superelevation transition was assumed to take place over 90, 110 and 200 feet (27.43, 33.53 and 60.96 m) for the 36, 30 and 10 degree curves with one-half of the superelevation transition occurring on the tangent section and half on the curve.

3. DISCUSSION OF RESULTS

3.1 Observational Data

3.1.1 38° Curve

As discussed in the Methodology Section, vehicle paths were defined as the lateral distance between the right rear tire of the vehicle and the right road edge. Negative values refer to distances off the road (i.e., vehicle traveling on shoulder). For the 38° curve, measurements were taken at 20 foot (6.1 m) intervals, starting 100 feet (30.5 m) before the Point of Curve (PC), and continuing 200 feet (61.0 m) into the curve. It should be recalled that this curve does not include a designed transition, but rather consists of a circular section following a tangent section. Table 2 presents the mean lateral offsets at each of the 16 points for each of the three specified vehicle types. Also presented are standard deviations assoicated with each of the means. These data are presented graphically in Figures 4, 5, and 6 Table 3 presents the mean speeds for each of the three vehicle types. Three speeds are given for each vehicle type, corresponding to the three 100 foot (30.5 m) intervals.

Table 2.

Mean Right Rear Wheel Displacement

38° Curve

Location on Curve* (feet)	Automobile Mean Displacement (feet)	Automobile Standard Deviation (feet)	School Bus Mean Displacement (feet)	School Bus Standard Deviation (feet)	Tractor-Trailer Mean Displacement (feet)	Tractor-Trailer Standard Deviation (feet)
-100	3.31	1.86	3.10	1.22	3.53	1.39
-80	3.61	1.81	3.26	1.22	3.77	1.39
-60	3.79	1.81	3.41	1.28	3.89	1.41
-40	3.92	1.73	3.52	1.09	3.95	1.41
-20	3.64	1.61	3.24	1.01	3.39	1.37
PC	2.82	1.48	2.27	1.00	2.13	1.47
+20	1.78	1.43	1.02	1.16	.43	1.73
+40	1.56	1.64	.17	1.58	-.74	2.12
+60	1.64	1.60	-.03	1.71	-.97	2.11
+80	1.93	1.59	-.03	2.16	-1.05	2.15
+100	2.09	1.81	-.03	2.24	-1.00	2.14
+120	2.03	1.66	.20	2.06	-.97	2.11
+140	2.03	1.76	.46	1.92	-1.06	2.04
+160	2.07	1.79	.40	2.09	-1.23	1.81
+180	1.68	1.49	.47	1.77	-1.19	1.55
+200	2.22	1.33	.61	1.78	-.90	1.37
N	30		30		30	

*Relative to PC
1 ft = 0.305 m

Table 3.

Mean Vehicle Speeds - 38° Curve

Location on Curve (feet)	Automobile Mean Speed (mph)	Automobile Standard Deviation (mph)	School Bus Mean Speed (mph)	School Bus Standard Deviation (mph)	Tractor-Trailer Mean Speed (mph)	Tractor-Trailer Standard Deviation (mph)
-100→PC	32.84	6.25	28.12	2.75	25.56	2.95
PC →+100	27.19	4.71	24.41	2.94	22.80	3.01
+100→+200	26.44	2.98	22.67	4.69	22.63	2.98

1 ft = 0.305 m
1 mph = 1.609 km/h

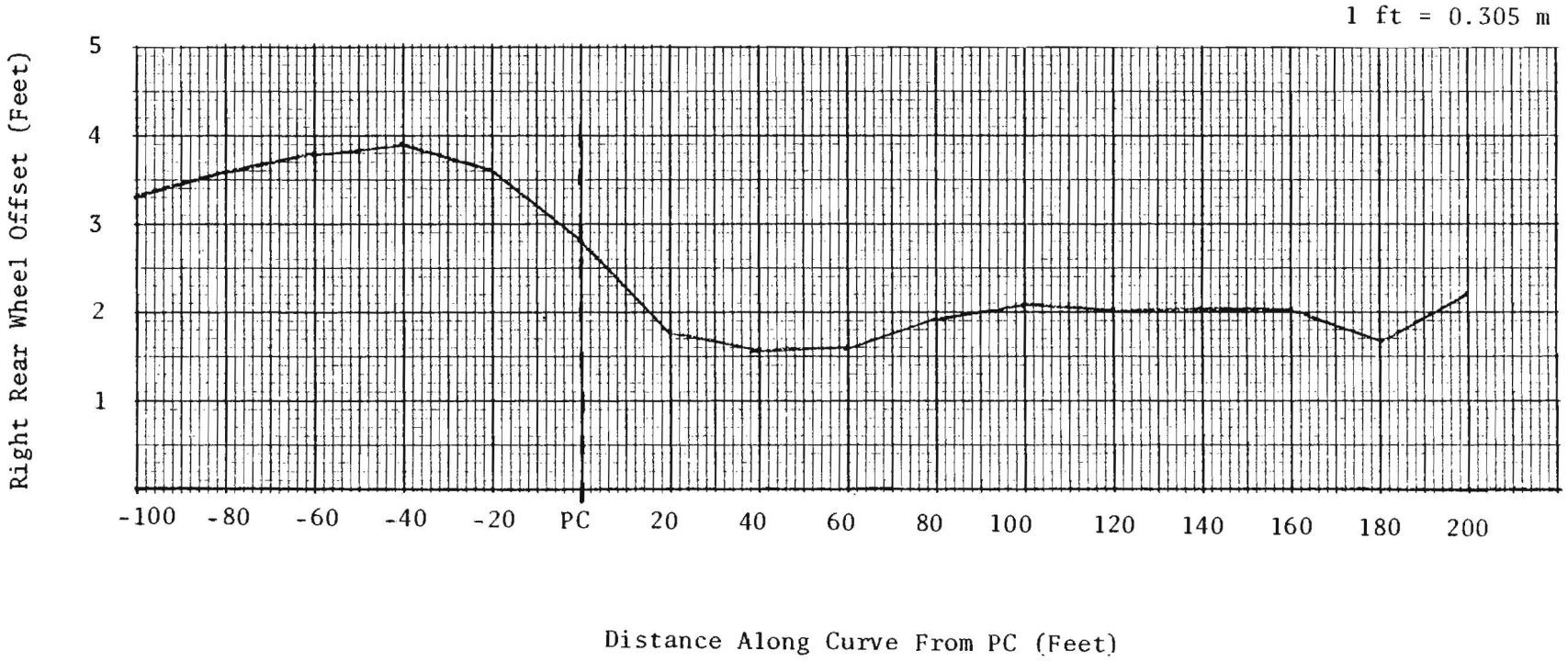

Figure 4. MEAN AUTO PATH 38° CURVE

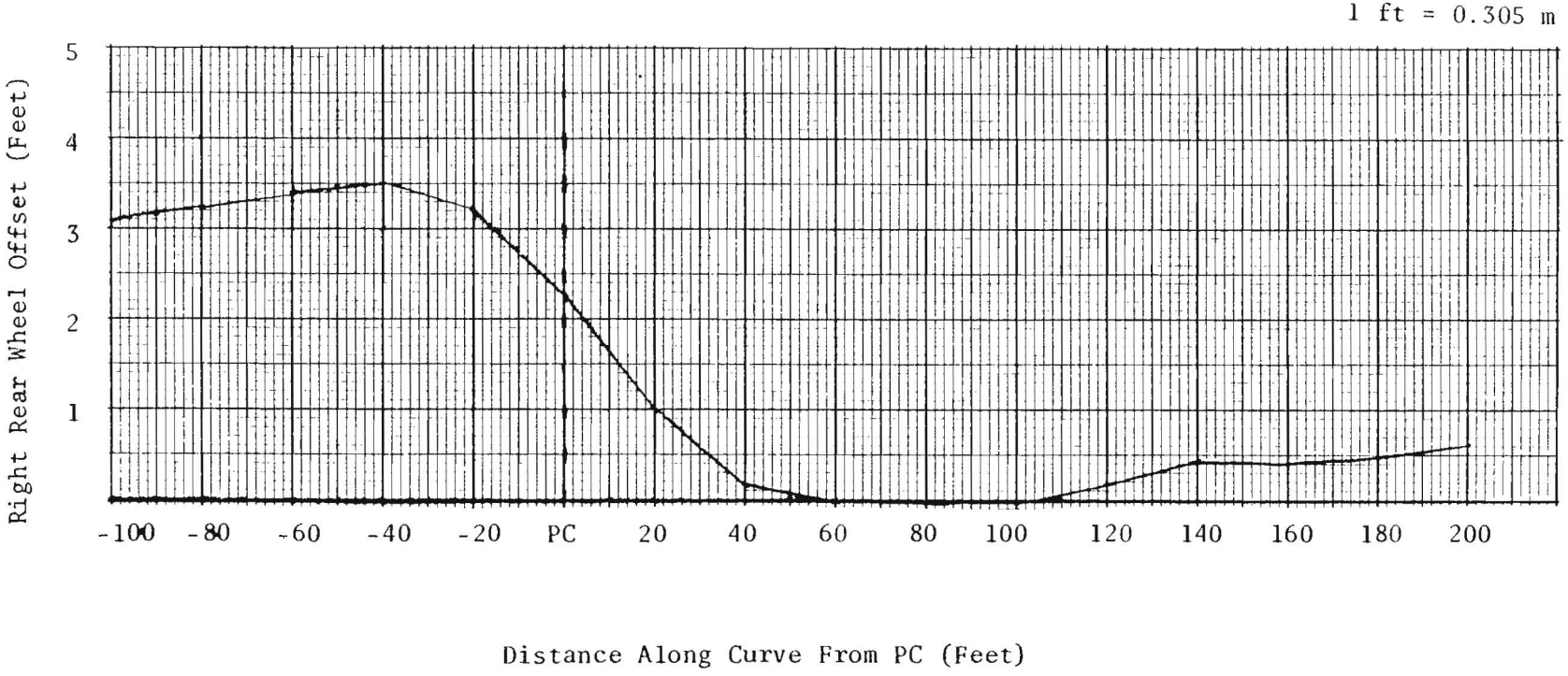

Figure 5. MEAN SCHOOL BUS PATH 38° CURVE

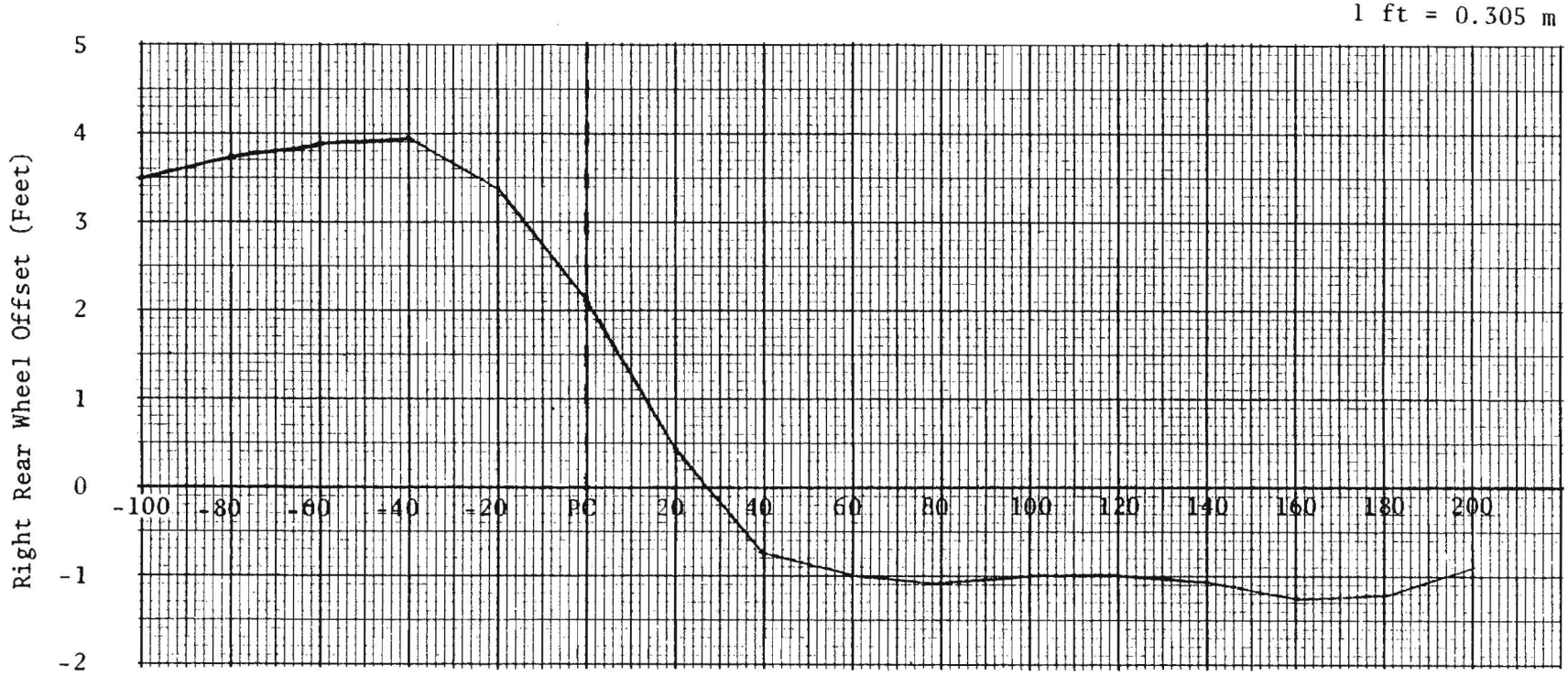

Figure 6. MEAN TRACTOR-TRAILER PATH 38° CURVE

Automobile Path

It is evident from Figure 4 that over the entire data collection interval of 300 feet (91.4 m), the lateral offset of the "average" automobile varies less than 2.5 feet (0.76 m). At no point along the interval does the path leave the roadway. In fact, of the 30 vehicle paths from which this mean path was calculated, only one automobile drove off the roadway during negotiation of this curve. That particular case appeared to be one of driver choice since the entire path was on the shoulder.

Of primary interest for the current study is the nature of the vehicle transition between the tangent road segment and the circular curve. The shape of the mean auto path suggests an interpretation involving the separation of the curve into three phases. Figure 7 presents the mean auto path divided into the following three hypothetical phases:

1) preparation
2) transition
3) curve following

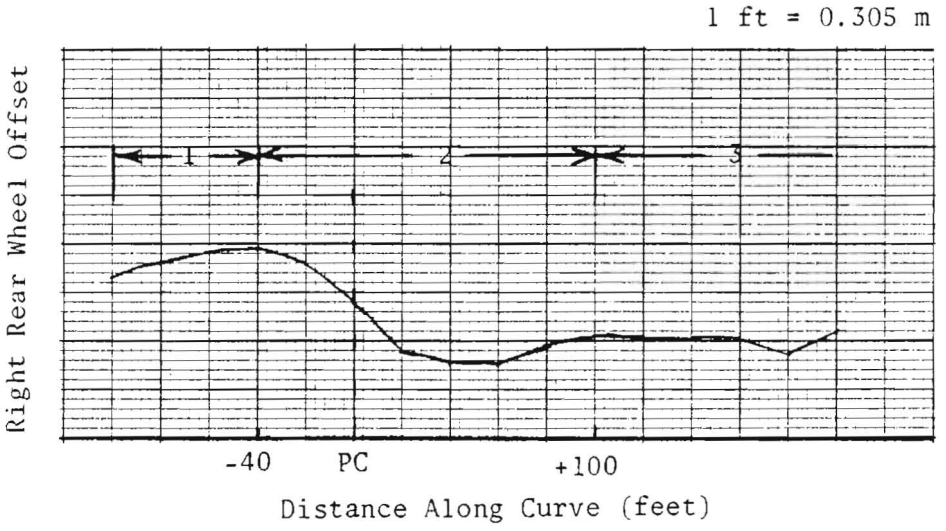

Figure 7. HYPOTHESIZED PHASES OF MEAN AUTO PATH 38° CURVE

The preparation begins at least 100 feet (30.5 m) before the PC, on the tangent road segment. It involves the driver moving slightly toward the center of the travel lane. This phenomenon is envisioned to be similar to preparations for turns at intersections or driveways in which a driver initially moves away from the turn in order to more easily negotiate the turn. As indicated in the figure, the mean preparation involves a change in position of less than one foot (0.305 m). The end of the preparation phase is defined as the point at which the driver/vehicle changes direction by turning the direction of the curve. On the graph, it is the maximum point (PC-40).

The second phase of the mean auto path will be referred to as the transition. This is defined to be the part of the path following the initial change in direction (maximum point on graph), and before the vehicle has attained a stable path which follows the curve. A stable path would be indicated graphically as a line parallel to the abcissa, which reflects a constant lateral offset. On the mean auto path presented in Figures 4 and 7 , the transition occurs over approximately 140 feet (42.7 m) including 40 feet (12.2 m) before the PC and 100 feet (30.5 m) of curve.

According to the graphs (Figures 4 and 7), the transition involves the vehicle moving closer to the road edge over a distance of 80 feet (24.4 m), followed by a move away from the road edge. Interpretation of this "reversal" should be made with caution. If this were a straight road segment, the move away from the road edge would imply a reversal in steering input. However, because the road at this point is curved, the graphic representation does not provide a meaningful indication of steering input. In fact, the continuation of the vehicle along a circular path through the transition would involve the vehicle first moving close to the road edge and then away from the road edge. This is shown schematically in Figure 8 . This figure presents a portion of a path which is an arc of a circle (the result of a constant steer angle). Figure 9 shows the transformation of a circular path into offset from the road edge. The mean auto path derived from the observational data is included for comparison. The circular path used for this figure was

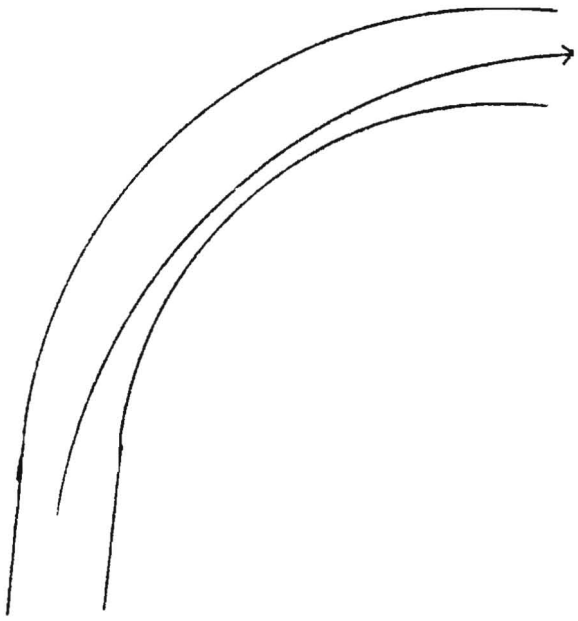

Figure 8. PATH ALONG CURVE WITH CONSTANT STEER ANGLE

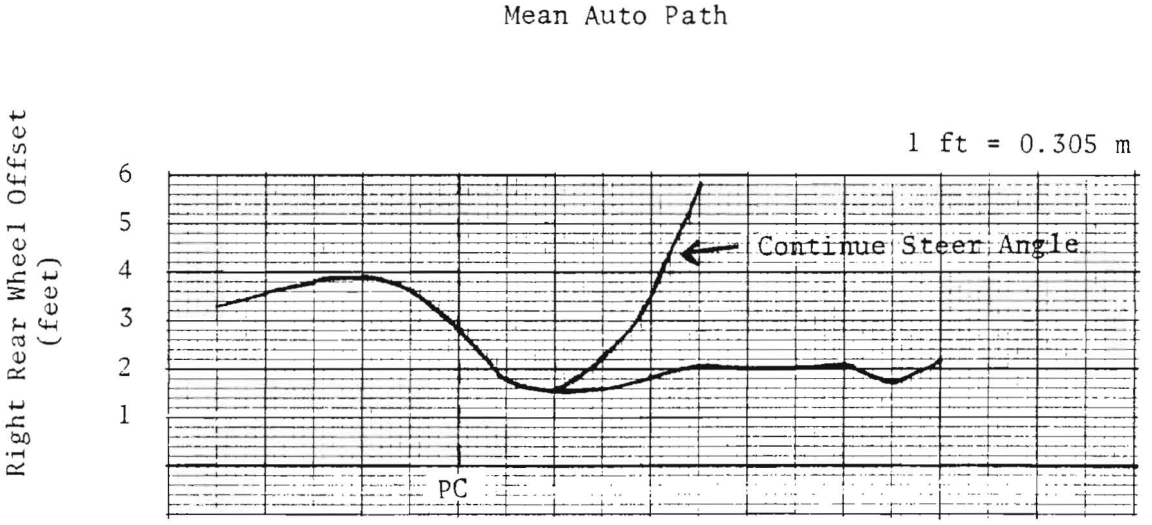

Figure 9. MEAN AUTO PATH WITH TRANSFORMATION OF CIRCULAR PATH RESULTING FROM A CONSTANT STEER ANGLE

generated from the observed mean offsets associated with the PC, PC +20, and PC +40. It shows that if the driver were to continue at a constant steer angle as selected at the PC (or before), the vehicle would move away from the road edge more quickly than was observed. Therefore, although the graph shows a move away from the road edge following the point at which the vehicle is closest to the road edge, the comparison with the circular path projected from the observed offsets at PC, PC +20, and PC +40, reveals that the "mean" driver is turning the vehicle further in the direction of the curve until he reaches a path which follows the given curve (at PC +100).

The third phase of the mean auto path is referred to as curve following. In this phase the driver maintains a constant offset from the road edge which implies that the vehicle is following the curve. This phase begins at approximately 90 feet (27.4 m) following the PC. At 160 feet (48.8 m) following the PC, the mean auto path shows a move closer to the road edge followed by a move away from the road edge. It is likely that this represents a preparation to merge. A number of observed vehicles moved away from the right road edge much sooner in preparation to merge with traffic.

Referring to Tables 2 and 3, it is evident that in the 100 feet (30.5 m) before the PC, the automobile paths exhibit more variability than do either school bus or tractor-trailer paths. Similarly, according to the mean speeds for the three vehicle types, automobiles approach the curve at the fastest speeds, and exhibit the most variability in approach speed. The change in mean speed between the first two 100 foot (30.5 m) intervals is largest for automobiles. All of these findings are consistant with the interpretation that auto drivers, perhaps aware of the relative responsiveness of their vehicles, need not adhere as strictly as drivers of other vehicles to a particular approach to the curve.

Hypothesis of Curve Following Behavior

Based upon the preceding analytical discussion of the mean auto path, a general hypothesis of how drivers/vehicles negotiate a transition from tangent to circular road segments can be formulated. The hypothesis is based upon the

assumption that it is desirable to reduce the lateral acceleration associated with such a curve and that one way to accomplish this reduction is to select a circular path corresponding to a degree of curvature less than that of the given curve. According to the hypothesis, the preparation phase is motivated by the intention of the driver to select a "less demanding" path through the curve. The preparation, which involves the vehicle moving away from the direction of the curve, has the function of placing the vehicle in a position where it is possible to select a path similar to that shown in Figure 8 The path shown in this figure is one of many possibilities from which the driver can select. The specific path selected by the driver is hypothesized to be determined in part by perceptual-motor skills of the driver, and in part by situation specific variables including environmental variables (road conditions) as well as driver variables (subjective tolerances, attention). It is obvious that some circular paths are more efficient than others, in terms of requiring additional corrections.

At some point along the curve, the initially selected circular path will become inadequate. At this point, additional steering inputs will be required by the driver in order to revise the path. Following this line of thought, the negotiation of the transition between tangent and circular segments is envisioned to involve a number of successive path revisions depending upon the efficiency of the individual path selections. This hypothesis allows any number of revisions. At one extreme is the situation as shown in Figure 8 in which the initially selected path allows the driver to successfully negotiate all but the very end of the curve. At the other extreme is the situation in which the driver is essentially continuously steering throughout the curve.

As stated, the hypothesis of curve following behavior is not particularly powerful in terms of predictive ability since it allows almost any behavior. It does, however, suggest the importance of determining the frequency of control inputs necessary for curve negotiation.

School Bus Path

In contrast to the mean auto path, reference to Figure 5 reveals that on the average, school buses used more of the road in order to negotiate the 38° curve. On the average, 3.5 feet (1.07 m) were used. The shape of the mean school bus path is similar to that associated with automobiles, suggesting that the same three phases (preparation, transition, curve following) can be used to describe the path. The primary difference between the two curves is that for the mean school bus path, the end of the transition phase and beginning of the curve following phase are confounded. It appears that on the average, the school bus would adopt a curve following mode more quickly than an auto driver, who perhaps is less constrained by the relationship between vehicle size and roadway geometrics.

Comparison of the standard deviations in Table 2 for school buses and autos reveals some differences. For example, during the preparation phase, on the straight road segment, the school bus paths exhibit less variability than do the auto paths. This may well reflect differences in vehicle width as well as the differences in vehicle handling. Following the PC, the variability associated with the school bus paths becomes greater than that associated with auto paths. This is interesting in that the reverse might be expected to be true. That is, it might be expected that because of smaller vehicle size, the automobiles would be less constrained to negotiate the curve in a particular way. This would be revealed as greater variability, which is not evident in the data.

Of the 30 sampled school buses, 9 (30%) selected a path which took the vehicle approximately 1 foot (0.305 m) off the road at some point in the data collection interval. Three (10%) selected paths in which the vehicle was approximately 5 feet (1.52 m) off the pavement onto the shoulder.

Referring once again to Table 3 , it is apparent that the mean school bus velocity for each of the three 100 foot (30.5 m) intervals is between the corresponding velocities for automobiles and tractor-trailers. The change in mean velocity over the three intervals is slightly smaller than that associated with automobiles. As evidenced by the standard deviations, the variability associated with the school bus velocities was smallest, relative to the other two vehicle types, in the first and second interval, and largest in the third.

Tractor-Trailer Path

Figure 6 presents the mean tractor-trailer path for the 38° Curve. As compared with the mean auto and mean school bus curve, it is apparent that on the average, tractor-trailers required more of the roadway in order to negotiate the curve. That is, over the entire data collection interval, the mean tractor-trailer path varied approximately 5.5 feet (1.68 m). Twenty-four (80 percent) of 30 tractor-trailers drove off the road at some point during the data collection interval. The shape of the mean tractor-trailer path is similar to the previous two curves with the exception of the magnitude of change in lateral position over the data collection interval. That is, like the mean auto and mean school bus, the mean tractor-trailer path can be characterized to include a preparation for the first 60 feet (18.3 m), followed by a transition which involves approximately 100 feet (30.5 m) of road. After the transition, the mean tractor-trailer path follows the curve, but with the right rear tire of the trailer on the shoulder of the road.

The nature of the transition associated with the mean tractor-trailer path differs slightly from that associated with the school bus and auto path in that the choice of path involves a sharper turn for tractor-trailers. This is evidenced by the fact that over the final 40 feet (12.2 m) of straight road prior to the PC, the change in lateral position for autos and school buses is approximately 1.1 to 1.2 feet (0.335 to 0.366 m), whereas the same change associated with the tractor-trailer path is approximately 1.8 feet (0.549 m). This

phenomenon is also shown by the point relative to the edge of the road, at which ease of the vehicle types assumes a curve following mode.

The standard deviations associated with the mean tractor-trailer path (Table 2) indicate that for tractor-trailers, the most variation in selection of path is associated with the transition, particularly on the curved segment, rather than the preparation phase. The distribution of individual standard deviations is similar to that for school buses in that smaller standard deviations were found during the preparation phase of the path. In additon, both school bus and tractor-trailer standard deviations increase as the vehicle gets into the transition and curve following phases. One difference between the two sets of standard deviations is that the school bus path exhibits the least amount of variability near the PC (s = 1.00). For tractor-trailers, the standard deviations are approximately the same for the entire interval before the PC.

The mean velocities for tractor-trailers (Table 3 .), were the smallest and involved the smallest change over the entire data collection interval. The standard deviations were essentially identical for the three intervals.

3.1.2 8° Curve

Of the three selected curves, the 8° curve was the only one to include a built-in transition between the tangent segment and circular curve. This was a 150 ft (45.7 m) spiral transition ($\Theta s = 6°$). For this curve, data were collected at 40 foot (12.2 m) intervals over a total of 480 ft (146.3 m) beginning approximately 70 feet (21.3 m) before the beginning of the spiral curve (TS), and ending 260 feet (79.2 m) into the circular curve. Table 4 presents the mean lateral displacement of the right rear wheel measured at each of the 13 points for each of the three vehicle types. The table includes a standard deviation for each calculated mean. These data are also presented graphically in Figures 10, 11, and 12.

Table 4.

Mean Right Rear Wheel Displacement

8° Curve

Point on Curve	Automobile		School Bus		Tractor-Trailer	
	Mean Displacement (feet)	Standard Deviation (feet)	Mean Displacement (feet)	Standard Deviation (feet)	Mean Displacement (feet)	Standard Deviation (feet)
0	3.75	.95	2.70	.69	2.57	.75
40	4.03	.92	3.05	.60	2.84	.74
80*	4.13	.97	3.13	.68	2.74	.87
120	4.01	1.06	2.95	.69	2.93	.91
160	3.41	1.08	2.32	.74	2.48	.95
200	2.52	1.16	1.78	.77	1.83	.84
240**	2.30	1.28	1.81	.80	1.81	.95
280	2.13	1.29	1.92	.84	1.85	1.09
320	2.25	1.40	1.99	1.02	2.10	1.06
360	2.22	1.44	2.08	1.08	2.23	1.19
400	2.32	1.52	2.16	1.11	2.32	1.17
440	2.31	1.56	2.27	1.16	2.44	1.15
480	2.52	1.64	2.41	1.07	2.45	1.21
N	30		13		20	

*TC is at 70
**PC is at 220
1 ft = 0.305 m

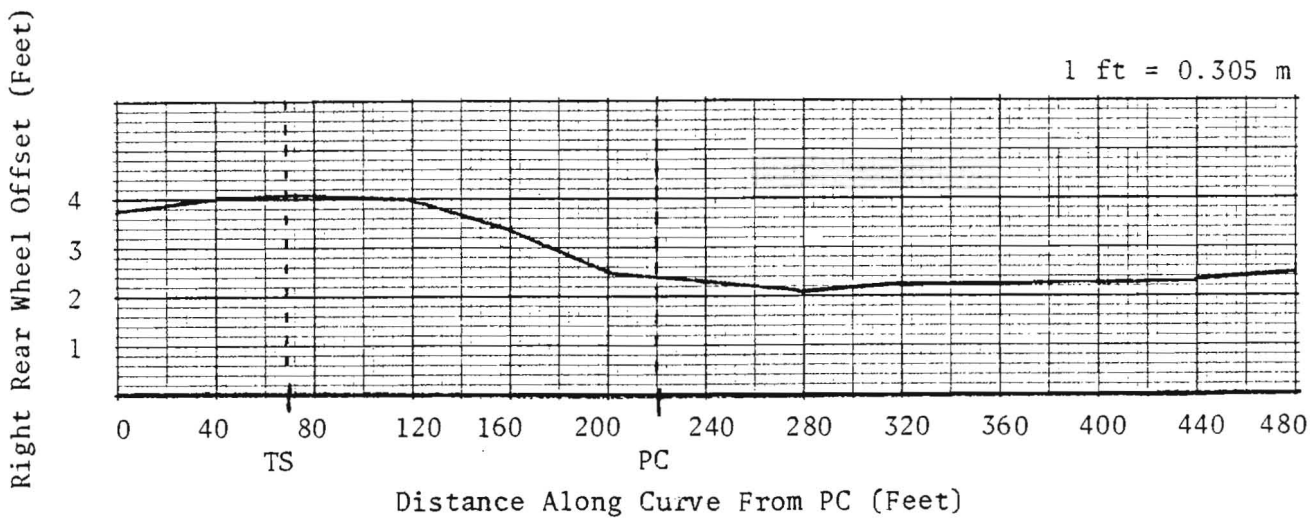

Figure 10. MEAN AUTO PATH 8° CURVE

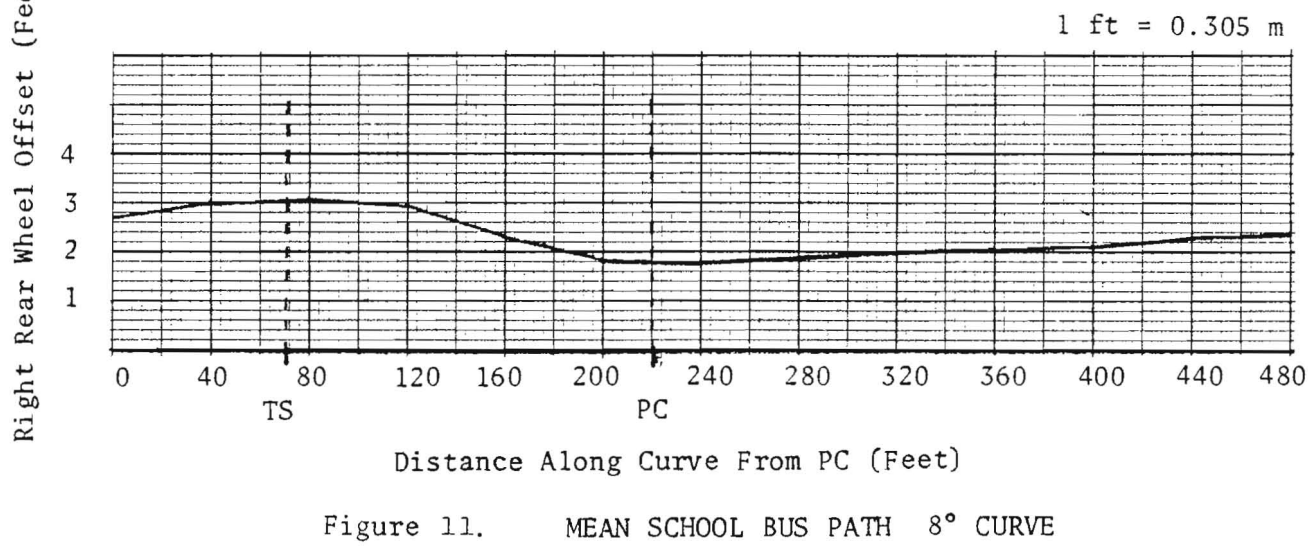

Figure 11. MEAN SCHOOL BUS PATH 8° CURVE

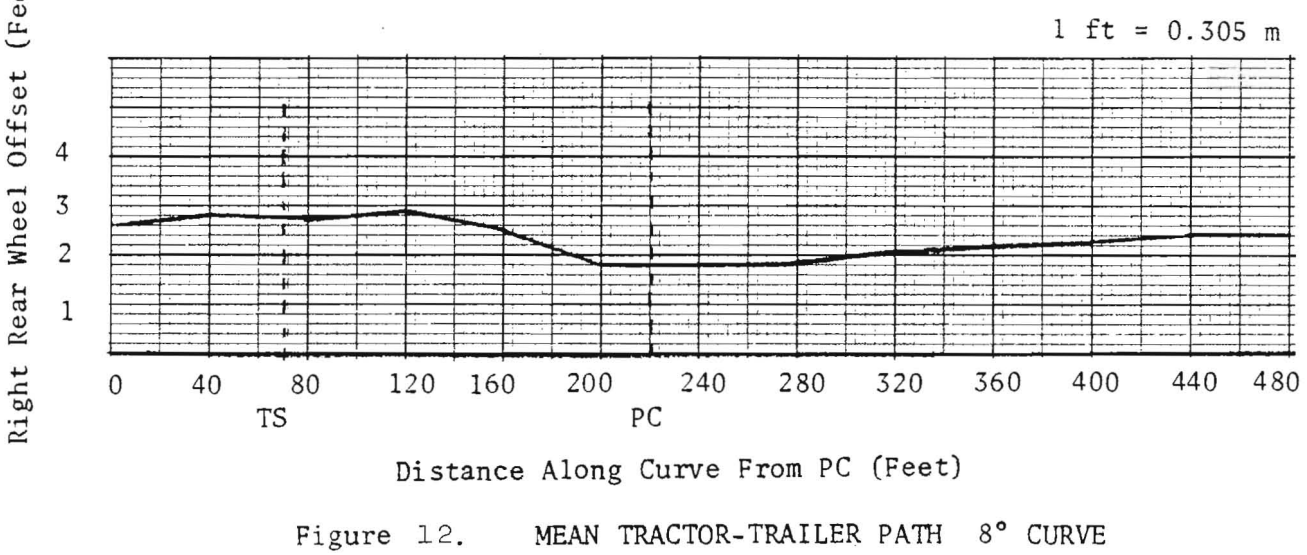

Figure 12. MEAN TRACTOR-TRAILER PATH 8° CURVE

It should be noted that the sample sizes of the vehicle types differ for this curve due to the relative scarcity of school bus and tractor-trailer traffic.

The mean velocities are presented in Table 5.

TABLE 5.

Mean Vehicle Speeds - 8° Curve

	Automobile		School Bus		Tractor-Trailer	
Location On Curve (feet)	Mean Speed (mph)	Standard Deviation (mph)	Mean Speed (mph)	Standard Deviation (mph)	Mean Speed (mph)	Standard Deviation (mph)
0-160	45.83	5.03	41.38	3.61	43.15	6.72
161-320	44.56	3.97	40.00	4.67	41.80	5.49
321-480	42.30	3.78	38.0	3.31	40.20	4.67

1 mph = 1.609 km/h

With regard to mean displacement plots shown in Figures 10, 11, and 12, it is notable that of the three paths the mean auto path involves the greatest variation in lateral placement, approximately 2 feet (0.61 m), over the entire data collection interval. This is in contrast to the results presented for the 38° curve which had the mean tractor-trailer path showing the greatest change in lateral placement over the entire data collection interval. For the 8° curve, as indicated in Figure 12 , the lateral position of the mean tractor-trailer varies only approximately 1 foot (0.305 m) over the entire interval.

In comparison with the graphs for the 38° curve, it appears that the three graphs for the 8° curve have a similar general shape. It is difficult to compare these three curves with those previously presented due to the existence of the spiral transition in the 8° curve. However, it does appear that prior to the spiral segment, the mean paths all exhibit a slight move away from the road edge which could be referred to as the preparation. Through the spiral road segment, all three mean paths exhibit a closer to the road edge,

which could again be referred to as a transition. The implication of this segment of the graphs is that the drivers all select a transition which is slightly different from the one built into the road. Although the graphs differ slightly in shape, it appears that at or slightly following the PC, the mean path for each of the three vehicle types has the vehicles following the curves. This is most apparent for the mean auto path. The mean school bus and tractor-trailer path suggest the selection of a slightly different curve throughout the circular road segment.

Concerning the standard deviations associated with the three mean paths for the 8° curve, it is apparent that automobiles exhibited the most variability in selection of path. According to an earlier discussion, this is what would be expected. The standard deviations for the mean auto path generally increase over the data collection interval. This is in contrast to those associated with the mean auto path for the 38° curve (see Table 2) for which standard deviations were fairly consistent throughout the data collection interval.

The standard deviations for both school buses and tractor-trailers tend to increase over the data collection interval. Relative to those associated with the 38° curve, the current standard deviations indicate less variability in the selection of path on the 8° curve.

As indicated in Table 5 , the mean velocities associated with the 8° curve are greater than those associated with the 38° curve (Table 3). In addition, the change in mean velocity over the data collection interval is approximately the same for each of the three vehicle types. In contrast to the velocity data for the 38° curve, the standard deviations are largest for tractor-trailers on the 8° curve. This may or may not be related to the finding that in contrast to the 38° curve, the mean tractor-trailer path on the 8° curve varied the least of the three vehicle types.

3.1.3 31° Curve

The 31° curve selected for observation, while generally similar to the 38° curve, differs in several ways. This curve had a much greater superelevation rate than the 38° curve. The 31° curve includes a slight upgrade while the 38° curve is essentially flat. Operationally, the 38° curve is an exit ramp, such that drivers, during negotiation of the curve, are preparing to merge with the traffic stream. The 31° curve is the first part of a compound curve which is an entrance ramp to a limited access roadway. At the point of data collection on the 31° curve, it is not necessary for the driver to be anticipating merging.

Data collection on the 31° curve was similar to that associated with the 38° curve in that the data were collected over 300 foot (91.4 m) interval using 20 foot (6.1 m) measurement intervals. Like the 38° curve, there is no built-in transition between the tangent and circular segments. Data, therefore, were collected on 100 feet (30.5 m) of straight road and 200 feet (61.0 m) of circular curve. Table 6 presents the mean lateral offsets and associated standard deviations for the three vehicle types on the 31° curve. The sample consists of 30 automobiles, 30 tractor-trailers, and 14 school buses. Figures 13, 14 and 15 present the offsets graphically and Table 7 gives the mean velocities for the curve.

Table 6.

Mean Right Rear Wheel Displacement

31° Curve

Point on Curve (ft)	Automobile		School Bus		Tractor-Trailer	
	Mean Displacement (feet)	Standard Deviation (feet)	Mean Displacement (feet)	Standard Deviation (feet)	Mean Displacement (feet)	Standard Deviation (feet)
-100	4.03	1.37	2.73	1.09	3.67	1.12
-80	4.09	1.28	2.74	1.08	3.72	1.14
-60	4.01	1.35	2.63	.99	3.76	1.17
-40	3.76	1.31	2.33	.94	3.61	1.23
-20	3.24	1.25	1.69	.91	3.11	1.25
PC	1.94	1.40	.43	1.16	1.97	1.24
+20	.69	1.53	-.87	1.63	.48	1.30
+40	.21	1.71	-1.29	2.07	-.26	1.39
+60	-.05	2.08	-1.44	2.45	-.57	1.52
+80	.01	2.02	-1.32	3.06	-.60	1.71
+100	-.09	2.00	-1.65	2.98	-.70	1.64
+120	-.14	2.22	-1.15	3.37	-.70	1.93
+140	.04	2.14	-1.35	3.52	-.66	2.00
+160	-.10	2.24	-1.63	3.64	-1.12	2.26
+180	.35	2.03	-1.26	3.66	-.63	2.09
+200	.27	2.04	-1.38	3.74	-.35	1.72
N	30		14		30	

1 ft = 0.305 m

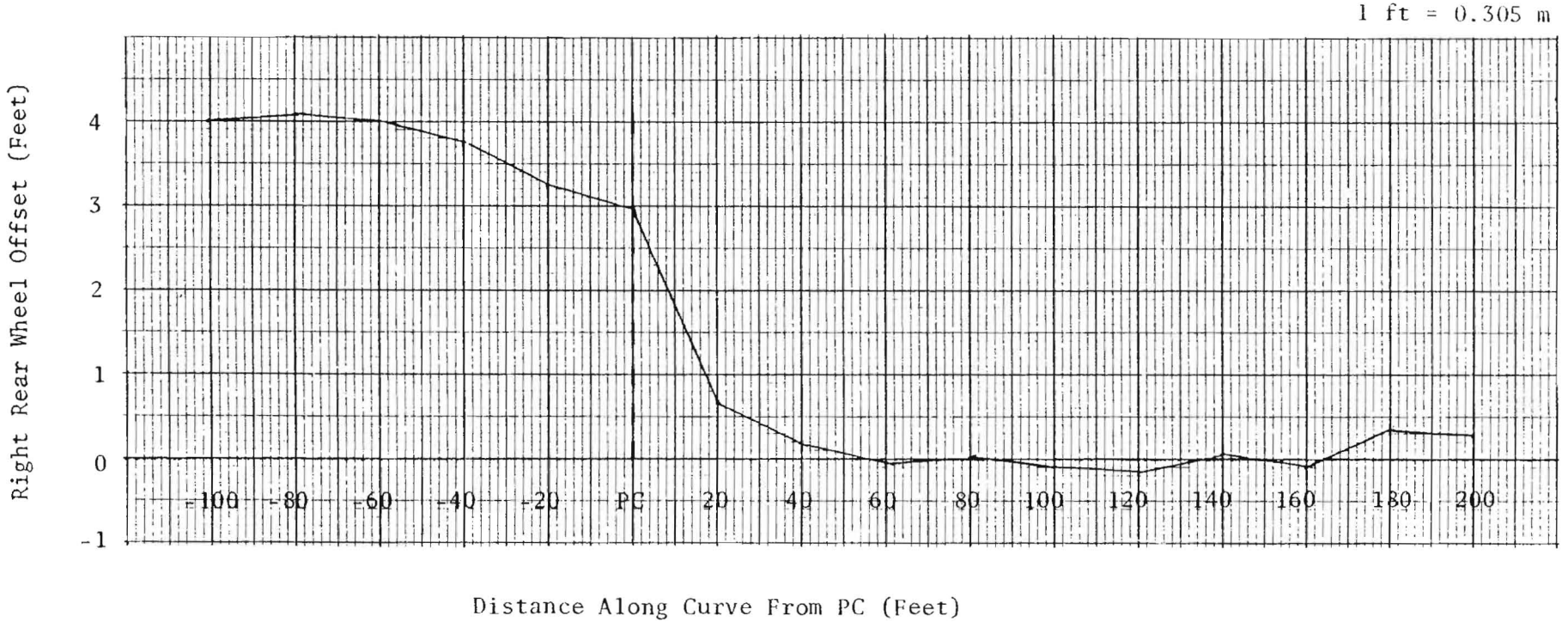

Figure 13. MEAN AUTO PATH 31° CURVE

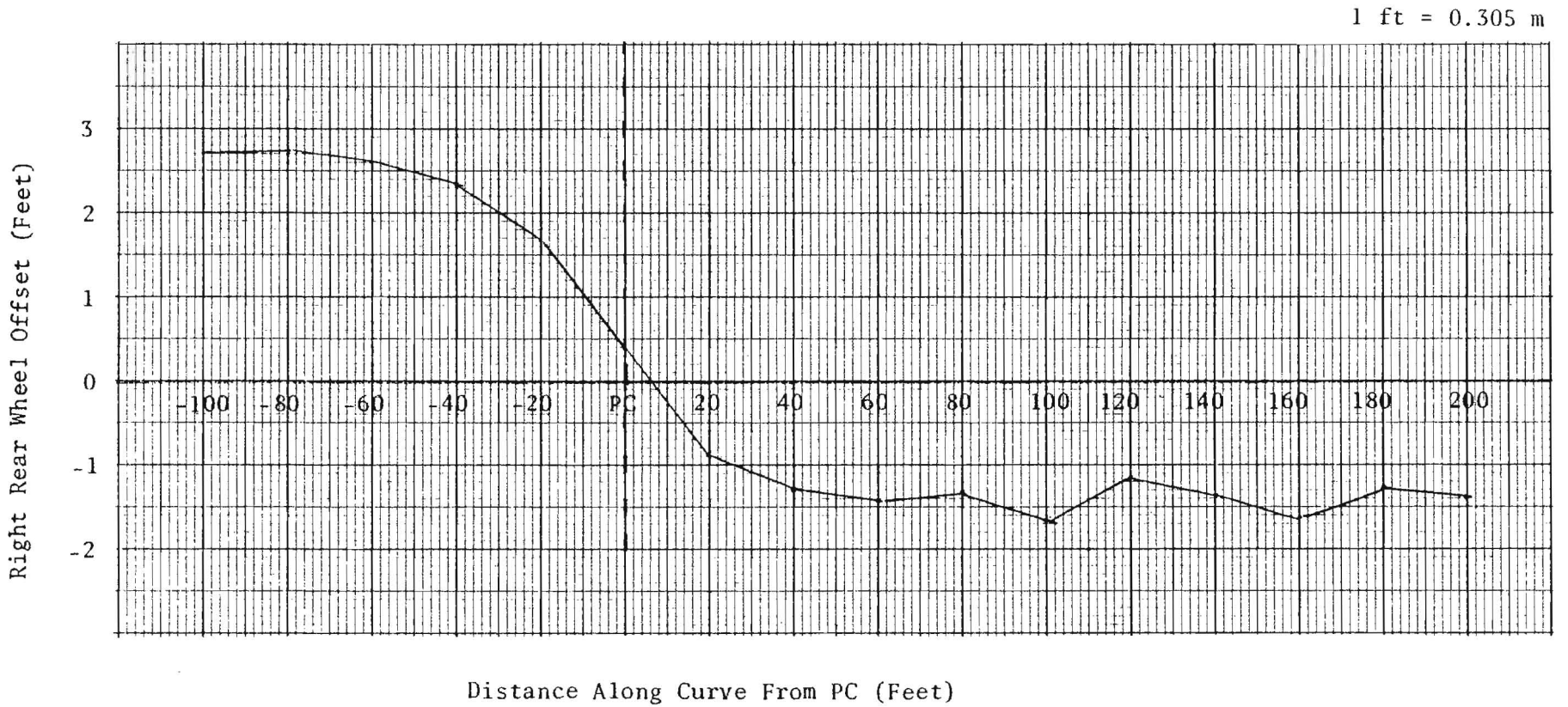

Figure 14. MEAN SCHOOL BUS PATH 31° CURVE

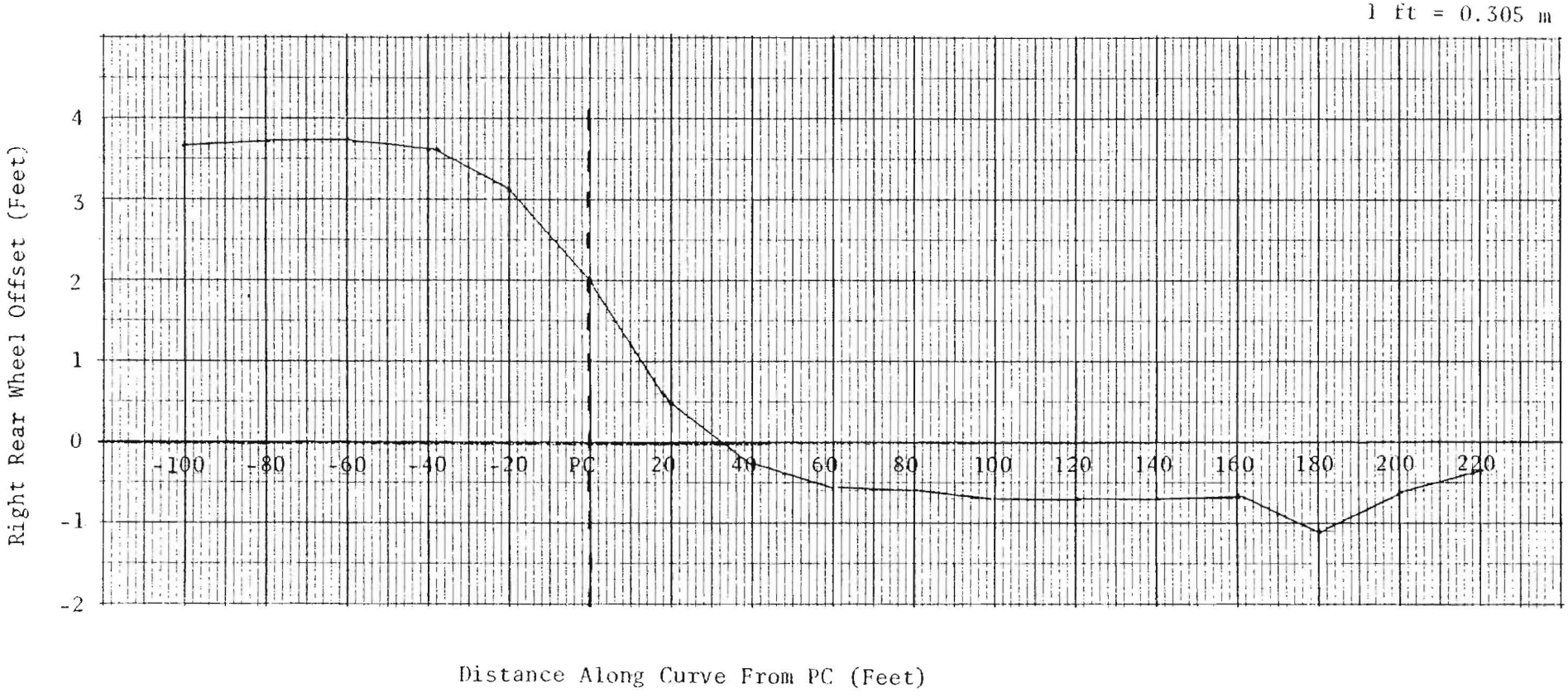

Figure 15. MEAN TRACTOR-TRAILER PATH 31° CURVE

Table 7.

Mean Vehicle Speeds - 31° Curve

Location On Curve (feet)	Automobile		School Bus		Tractor-Trailer	
	Mean Speed (mph)	Standard Deviation (mph)	Mean Speed (mph)	Standard Deviation (mph)	Mean Speed (mph)	Standard Deviation (mph)
-100 to PC	29.70	2.89	26.28	1.58	24.26	2.31
PC to 100	27.23	2.66	26.28	1.58	23.83	2.19
100 to 200	28.63	3.11	27.42	1.15	25.06	2.49

1 mph = 1.609 km/h

The highest proportion of vehicles traveling on the shoulder during a portion of the data collection interval was observed on the 31° curve. Of 30 autos, 17 (57 percent) drove on the shoulder at some point during the data collection interval. The corresponding proportions for school buses and tractor-trailers were 79 percent and 73 percent, respectively. As is evident in Figures **13** , **14** , and **15** , all three of the mean paths involve departures from the travel lane at some point along the curve.

The mean paths for this curve differ from those discussed previously in that prior to the transition, the paths do not involve preparatory moves away from the road edge. The transition and curve following phases appear quite similar to those for the 38° curve in terms of the general shapes of offset as plotted.

The standard deviations associated with the mean lateral offsets tend to increase along the length of the curve, indicating that paths were more uniform before and early in the curve. Of the three curves, the variability among the individual vehicles was greatest for this curve, particularly for school buses.

In contrast to the large standard deviations associated with lateral placements, the speeds for this curve were more uniform than for the other two curves. In addition, the changes in mean speeds for the three vehicle types were smallest for this curve. In fact, all three vehicle types revealed an increase in mean speed between the second and third 100 foot (30.5 m) segment.

3.1.4 Discussion

The analysis of path data has been based upon paths derived from mean lateral displacements. There exists, however, some concern regarding the interpretation of these results. The discussions heretofor have treated these mean paths as if they were "representative" paths. However, magnitudes of the standard deviations of the mean offsets indicate a possible lack of reliability associated with these mean paths.

As an example, two individual automobile paths for the 38° curve are presented in Figures 16 and 17.

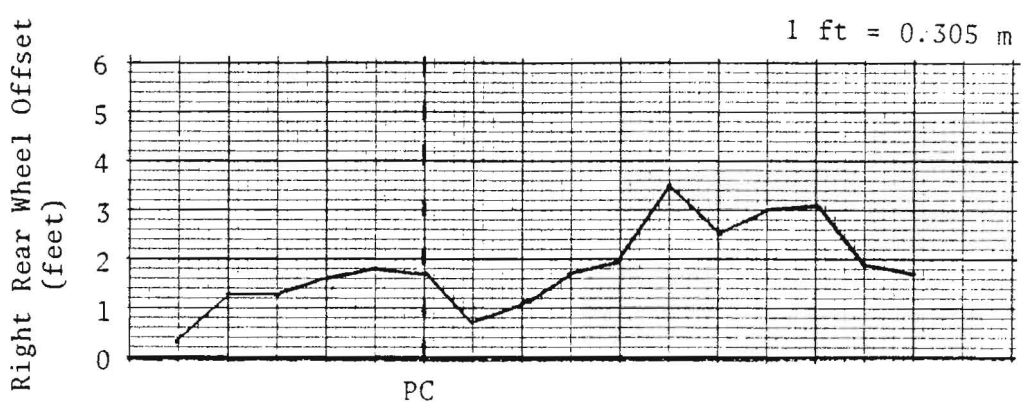

Figure 16. INDIVIDUAL AUTO PATH 38° CURVE
(Auto 15)

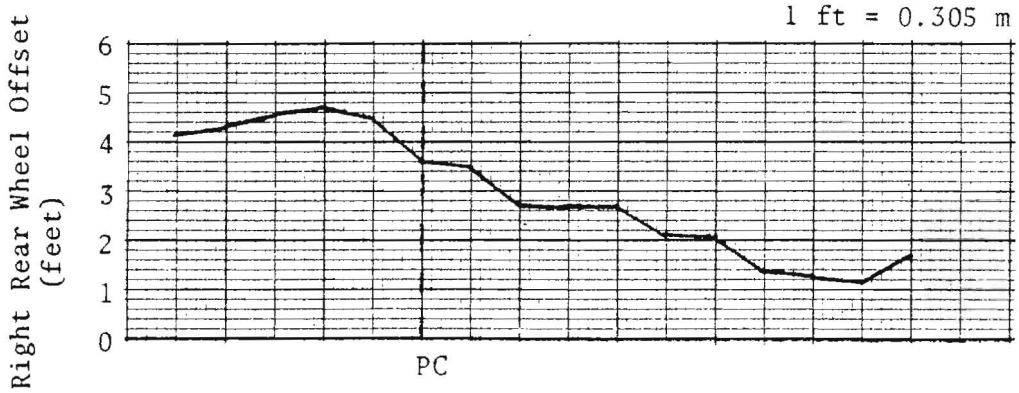

Figure 17. INDIVIDUAL AUTO PATH 38° CURVE
(Auto 16)

It is obvious that both curves reflect driver/vehicle behavior different from that suggested by the mean auto path for the 38° curve (Figure 4). In the previous discussion of the mean path, it was suggested that 3 phases exist (preparation, transition, curve following). These two figures, however, reveal the ambiguity associated with an attempted separation into three discrete phases. Both of the individual paths appear to include a preparatory move away from the road followed by a transition involving a move in the curve direction. However, neither of these individual graphs involve a stabilization or curve following mode. Rather, it appears that both vehicles are changing path throughout the data collection interval.

The analysis has also neglected the possibility of an interaction between path selection and velocity. Such a relationship was addressed peripherally in the discussion of similarities between the distributions of standard deviations for speed and lateral position on the roadway. However, no systematic treatment of this interaction was attempted. Figures 18 and 19 present two individual automobile paths for the 31° curve. Superimposed on the graphs are the calculated velocities associated with the three 100 foot (30.5 m) intervals. These two paths apparently reveal different priorities for the negotiation of the subject curve. The first vehicle (Auto #7) approached the curve at a speed of 27 mph (43.4 km/h). It appears that the driver placed a high priority on maintaining a relatively constant offset, that is, to accurately follow the curve. To accomplish this, a moderate approach speed, followed by a change in speed of 3 mph (4.83 km/h), was required. The other automobile (Auto #31) apparently intended to maintain a relatively high speed throughout the data collection interval. If one can assume this intention, it is apparent from Figure 19 that in order to maintain the relatively high speed, the driver was required to select a path, involving a relatively large deviation from the given curve, which represents a larger radius than the designed curve.

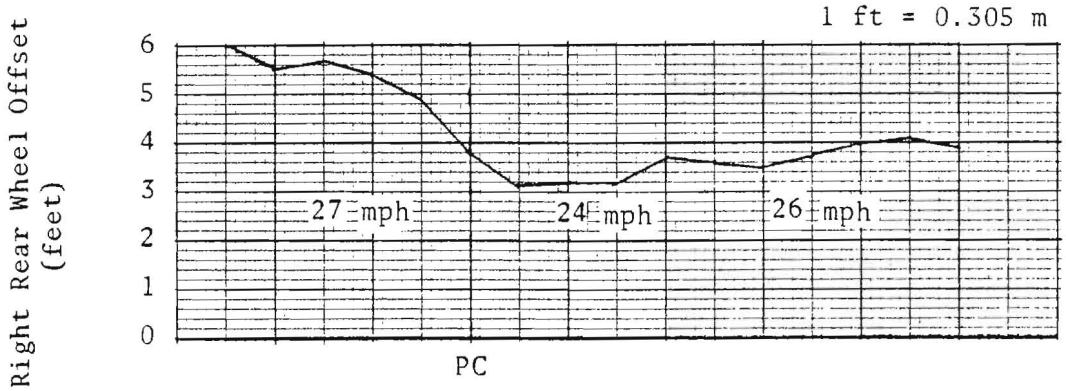

Figure 18. INDIVIDUAL AUTO PATH 38° CURVE
(Auto 7)

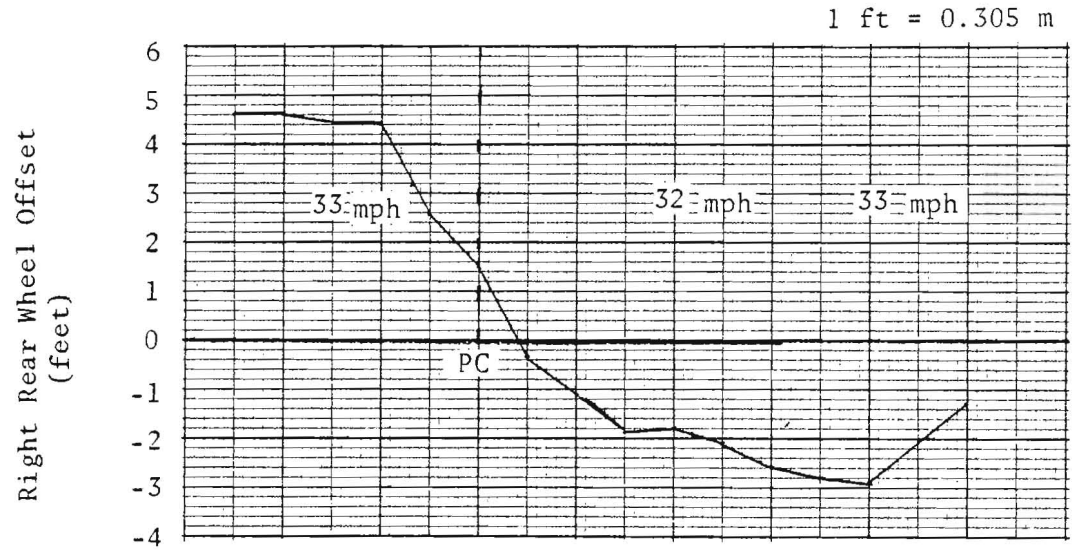

Figure 19. INDIVIDUAL AUTO PATH 38° CURVE
(Auto 31)

3.2 Simulation Results

3.2.1 Literature Search

A search of the available literature on articulated vehicle simulations was undertaken in order to determine whether such a simulation was in existence that would be applicable to the task of considering the vehicle negotiating superelevated horizontal curves.

Articulated vehicle models of varying complexity have been developed by a number of researchers in the field of vehicle dynamics. Many early efforts involved analysis of lateral stability with simplified representations of the vehicle (for example, References 8, 9 and 10). More recent analyses and subsequent computer simulations have extended the earlier work into the nonlinear range. Among the more significant contributions are References 12 through 15.

While these references do describe articulated vehicle models that might ultimately be of value in a program studying curve design criteria, they all lack the necessary capability for considering the effects of superelevation (that is, varying terrain elevation and slope). Snelgrove did indicate that an articulated vehicle research program at the Ministry of Transport in Ontario, Canada was planned to modify the articulated vehicle simulation developed at the Highway Safety Research Institute so that superelevated curves could be considered (Reference 16). However, as a result of correspondence with Mr. Snelgrove, it was learned that these plans were abandoned due to the extensive modifications that would be required to that simulation.

Consequently, no articulated vehicle simuations were available with the capabilities required for this research program.

3.2.2 Simulation Study

A simulation run matrix consisting of:

- 3 vehicles
- 3 vehicle speeds
- 3 circular curves
- 3 tangent to curve transitions
- 2 superelevations

was employed for this investigation of horizontal curve design requirements. The elements of this run matrix were:

- vehicles: compact automobile
  full size automobile
  school bus
- circular curves: 36°
  30°
  10°
- transitions: spiral
  compound circular
  none
- superelevations: 8%
  12%
- vehicle speeds: design speed
  design speed + 20%
  design speed - 20%.

As noted in Section 2.2, the design speed varied as a function of the degree of curve (or curve radius). The design speeds used for the three curves studied were:

Curve	Design Speed mph	(km/h)
36°	25.7	(41.4)
30°	28.6	(46.0)
10°	46.4	(74.7)

The simulation run schedule was organized into 27 run series with 6 runs within each series. The six runs within each series were used to investigate the effects of superelevation and vehicle speed on results for a given curve, curve transition and vehicle as follows:

Run Series-No.	Speed	Superelvation - %
-1	Design	8
-2	Design + 20%	8
-3	Design - 20%	8
-4	Design	12
-5	Design + 20%	12
-6	Design - 20%	12

The series run schedule used in the study is given in Table 3

Results were summarized by tabulating characteristics of the command steer time histories as illustrated in Figure 20. Items summarized include:

- maximum steer rate (reflected to the steering wheel assuming overall steering ratios of 20:1 and 30:1 for the automobiles and school bus, respectively)
- front wheel steer angle overshoot
- maximum front wheel steer angle oscillation amplitude
- number of cycles required to damp out steer oscillation
- steady-state front wheel steer angle.

Table 8. SIMULATION RUN SERIES SCHEDULE

Run Series	Vehicle	Curve	Transition
I	Compact	36°	Spiral
II	Full Size	36°	Spiral
III	School Bus	36°	Spiral
IV	Compact	36°	None
V	Full Size	36°	None
VI	School Bus	36°	None
VII	Compact	36°	Compound
VIII	Full Size	36°	Compound
IX	School Bus	36°	Compound
X	Compact	30°	Spiral
XI	Full Size	30°	Spiral
XII	School Bus	30°	Spiral
XIII	Compact	30°	None
XIV	Full Size	30°	None
XV	School Bus	30°	None
XVI	Compact	30°	Compound
XVII	Full Size	30°	Compound
XVIII	School Bus	30°	Compound
XIX	Compact	10°	Spiral
XX	Full Size	10°	Spiral
XXI	School Bus	10°	Spiral
XXII	Compact	10°	None
XXIII	Full Size	10°	None
XXIV	School Bus	10°	None
XXV	Compact	10°	Compound
XXVI	Full Size	10°	Compound
XXVII	School Bus	10°	Compound

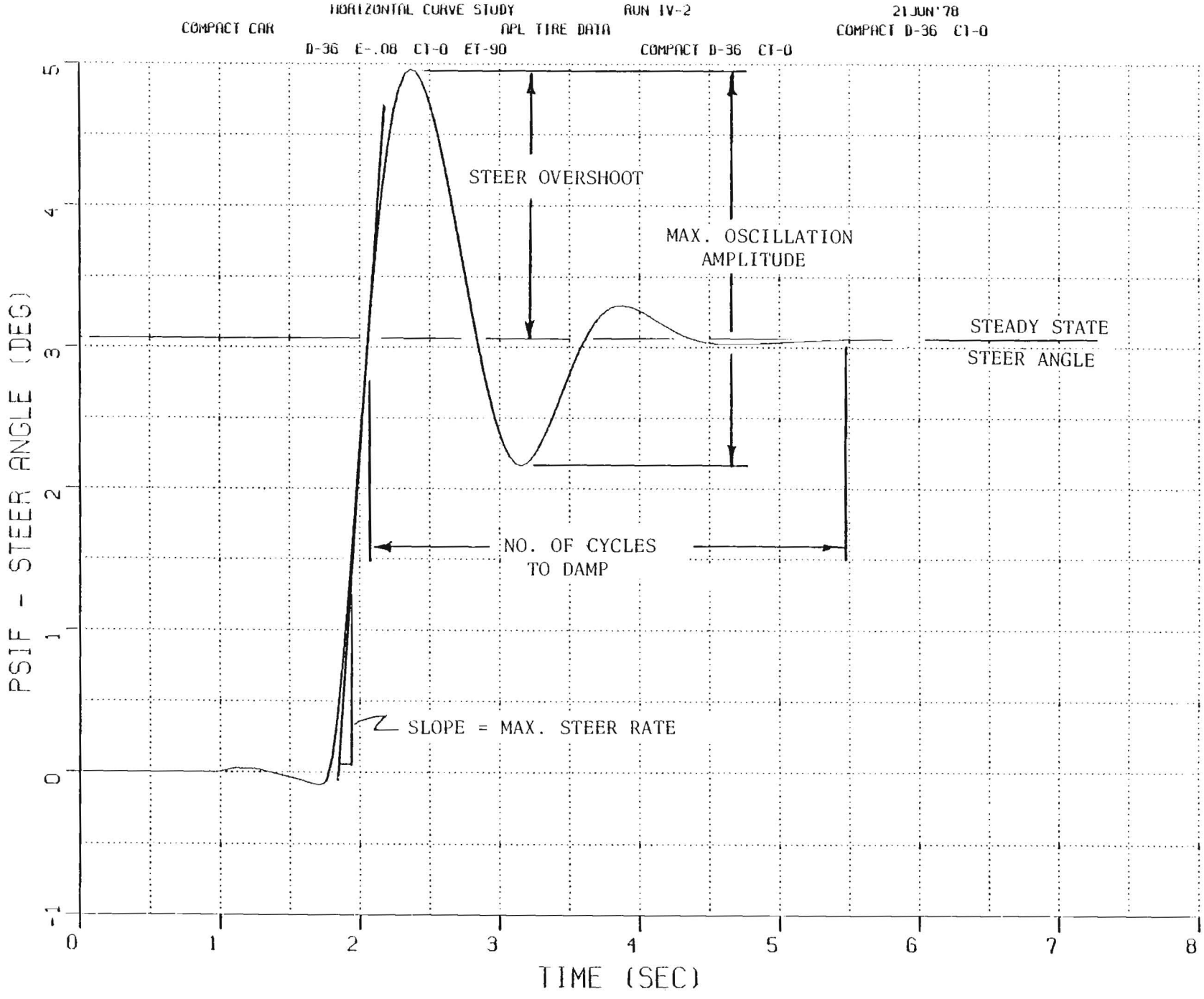

Figure 20. STEER CHARACTERISTICS

Also tabulated are:

- maximum transient lateral acceleration
- steady-state lateral acceleration
- steady-state vehicle slip angle
- right rear wheel offset from the path centerline.

Summary tabulations extracted from the computer runs are given in Table 9 . In extracting the number of cycles necessary to damp out any steer overshoot, it was arbitrarily assumed that front wheel angular deviations of $\pm$ 0.05° ($\approx$ 1° at the steering wheel) did not constitute a meaningful amplitude and were thus not counted.

Table 9 does not contain summaries of results of vehicles traversing the 10 degree curve with a spiral transition. Results from these cases were not obtained due to problems encountered with the automatic guidance algorithm. The causes of these problems are not definitely known but are believed to be associated with difficulties in resolving small path errors during the spiral transition. The determination of a steer command error (i.e., the distance between the guide point fixed to the vehicle and the spiral curve measured along a normal to the vehicle x-axis) requires an iterative procedure because the location of a point along the spiral can only be found by solving two parametric integral equations. In establishing the proper position for a point on the spiral for calculation of the steer command, error limits are set within the algorithm to accept a location on the spiral if it is close to the point which is normal to the vehicle x-axis (i.e., the exact point). However, when the steering error (i.e., the distance from the vehicle guide point to the spiral) is small, the error limit on the spiral point determination is large in relation to it. When this occurs, discontinuous variations in steering commands can occur.

Table 9. SUMMARY OF SIMULATION RESULTS

RUN NUMBER	MAXIMUM STEERING WHEEL RATE	FRONT WHEEL			MAXIMUM LATERAL ACCEL.	STEADY STATE			
		STEER OVERSHOOT	MAXIMUM OSCILLATION AMPLITUDE	NO. CYCLES TO DAMP		LATERAL ACCEL.	FR WHEEL STEER ANGLE	RR WHEEL OFFSET	BODY SLIP ANGLE
	DEG/SEC	DEG	DEG	-	G's	G's	DEG	IN	DEG
I-1	30.0	0.09	0.10	0.5	0.28	0.27	2.99		0.04
I-2	42.8	0.36	0.36	0.5	0.40	0.38	3.05	-24.2	-0.87
I-3	19.2	0.02	0.02	-	0.18	0.18	2.92	-29.9	0.79
I-4	25.0	0.10	0.10	0.5	0.28	0.27	2.95	-28.3	0.33
I-5	40.0	0.27	0.27	0.5	0.40	0.38	3.02	-25.2	-0.56
I-6	19.2	0.02	0.02	-	0.18	0.18	2.88	-30.8	1.08
II-1	34.0	0.09	0.09	0.5	0.28	0.27	3.79	-31.4	0.79
II-2	46.4	0.34	0.34	0.5	0.40	0.38	3.95	-27.5	-0.04
II-3	25.2	0.03	0.03	-	0.18	0.18	3.70	-34.6	1.48
II-4	32.6	0.08	0.08	0.5	0.28	0.27	3.74	-32.6	1.06
II-5	45.2	0.25	0.25	0.5	0.40	0.38	3.89	-28.8	0.25
II-6	25.2	0.02	0.02	0.5	0.19	0.18	3.67	-35.6	1.74
III-1	91.5	0.03	0.03	-	0.27	0.27	7.33	-63.0	1.59
III-2	119.4	0.34	0.34	0.5	0.39	0.37	7.27	-54.0	0.73
III-3	70.2	-	-	-	0.18	0.18	7.40	-67.0	2.23
III-4	90.6	-	-	-	0.28	0.28	7.37	-63.5	1.82
III-5	119.4	0.17	0.17	0.5	0.40	0.38	7.29	-57.0	1.03
III-6	69.6	-	-	-	0.19	0.18	7.41	-68.5	2.44

1 in = 25.4 mm

Table 9. (Continued)

RUN NUMBER	MAXIMUM STEERING WHEEL RATE	FRONT WHEEL			MAXIMUM LATERAL ACCEL.	STEADY STATE			
		STEER OVERSHOOT	MAXIMUM OSCILLATION AMPLITUDE	NO. CYLCES TO DAMP		LATERAL ACCEL.	FR WHEEL STEER ANGLE	RR WHEEL OFFSET	BODY SLIP ANGLE
	DEG/SEC	DEG	DEG	-	G's	G's	DEG	IN	DEG
IV-1	190.0	0.90	1.12	1.0	0.31	0.27	3.00	-27.2	0.01
IV-2	258.0	1.90	2.79	1.5	0.49	0.37	3.06	-24.1	-0.88
IV-3	126.0	0.26	0.33	1.0	0.19	0.18	2.92	-29.9	0.79
IV-4	192.0	0.90	1.10	1.0	0.31	0.27	2.94	-28.4	0.35
IV-5	260.0	1.83	2.63	1.5	0.48	0.38	3.02	-25.3	-0.55
IV-6	126.0	0.25	0.33	1.0	0.19	0.17	2.87	-30.9	1.08
V-1	170.0	0.60	0.70	1.0	0.30	0.27	3.78	-31.5	0.78
V-2	230.0	1.53	1.94	1.0	0.46	0.37	3.94	-27.8	-0.08
V-3	116.0	0.06	0.09	1.0	0.18	0.18	3.71	-34.6	1.49
V-4	168.0	0.55	0.67	1.0	0.30	0.27	3.74	-32.7	1.07
V-5	230.0	1.46	1.88	1.0	0.46	0.38	3.86	-28.9	0.24
V-6	118.0	0.05	0.11	1.0	0.18	0.18	3.67	-35.7	1.75
VI-1	198.0	0.08	0.12	1.0	0.29	0.27	7.36	-64.0	1.58
VI-2	276.0	0.64	0.94	1.0	0.44	0.37	7.30	-54.0	0.75
VI-3	144.0	-	-	-	0.18	0.18	7.40	-64.5	2.24
VI-4	204.0	0.02	0.06	1.0	0.28	0.28	7.36	-64.0	1.83
VI-5	276.0	0.40	0.60	1.0	0.44	0.38	7.31	-54.0	1.03
VI-6	138.0	-	-	-	0.18	0.18	7.39	-68.0	2.44

1 in = 25.4 mm

Table 9. (Continued)

RUN NUMBER	MAXIMUM STEERING WHEEL RATE	FRONT WHEEL			MAXIMUM LATERAL ACCEL.	STEADY STATE			
		STEER OVERSHOOT	MAXIMUM OSCILLATION AMPLITUDE	NO. CYCLES TO DAMP		LATERAL ACCEL.	FR WHEEL STEER ANGLE	RR WHEEL OFFSET	BODY SLIP ANGLE
	DEG/SEC	DEG	DEG	-	G's	G's	DEG	IN	DEG
VII-1	96.0	0.48	0.56	1.0	0.29	0.27	3.00	-27.2	0.02
VII-2	132.0	1.00	1.31	1.5	0.44	0.37	3.06	-24.8	-0.99
VII-3	64.0	0.15	0.5	0.5	0.18	0.18	2.91	-29.8	0.77
VII-4	94.0	0.42	0.47	1.0	0.29	0.27	2.95	-28.3	0.35
VII-5	132.0	0.95	1.18	1.5	0.43	0.38	3.00	-25.1	-0.64
VII-6	64.0	0.12	0.14	0.5	0.18	0.18	2.89	-30.8	1.06
VIII-1	84.0	0.31	0.33	0.5	0.29	0.27	3.79	-31.4	0.78
VIII-2	118.0	0.78	0.91	1.0	0.42	0.38	3.95	-27.5	-0.04
VIII-3	58.0	0.04	-	-	0.18	0.18	3.71	-34.5	1.48
VIII-4	84.0	0.29	0.31	0.5	0.29	0.28	3.74	-32.6	1.07
VIII-5	118.0	0.71	0.85	1.0	0.43	0.38	3.89	-28.8	0.23
VIII-6	58.0	0.03	0.04	-	0.19	0.18	3.68	-35.7	1.74
IX-1	105.0	0.03	0.04	-	0.28	0.28	7.38	-64.0	I.58
IX-2	141.0	0.37	0.47	1.0	0.42	0.38	7.25	-50.8	0.74
IX-3	75.0	-	-	-	0.18	0.18	7.40		2.24
IX-4	105.0	0.04	0.04	-	0.29	0.28	7.38	-64.0	1.84
IX-5	144.0	0.28	0.33	1.0	0.40	0.38	7.26	-57.0	1.02
IX-6	78.0	-	-	-	0.19	0.18	7.40	≈-70.0	2.45

1 in = 25.4 mm

Table 9. (Continued)

RUN NUMBER	MAXIMUM STEERING WHEEL RATE	FRONT WHEEL			MAXIMUM LATERAL ACCEL.	STEADY STATE			
		STEER OVERSHOOT	MAXIMUM OSCILLATION AMPLITUDE	NO. CYLCES TO DAMP		LATERAL ACCEL.	FR WHEEL STEER ANGLE	RR WHEEL OFFSET	BODY SLIP ANGLE
	DEG/SEC	DEG	DEG	-	G's	G's	DEG	IN	DEG
X-1	24.0	0.15	0.17	0.5	0.29	0.28	2.52	-26.3	-0.29
X-2	40.0	0.34	0.40	1.0	0.42	0.38	2.59	-23.0	-1.24
X-3	16.0	0.03	0.03	-	0.18	0.18	2.44	-29.1	0.50
X-4	24.0	0.11	0.12	0.5	0.29	0.28	2.48	-27.4	0.02
X-5	30.0	0.27	0.29	0.5	0.41	0.39	2.56	-24.1	-0.90
X-6	16.0	0.02	0.03	-	0.19	0.18	2.41	-29.9	0.79
XI-1	32.0	0.11	0.12	0.5	0.29	0.28	3.19	-29.9	0.37
XI-2	44.0	0.34	0.36	0.5	0.41	0.38	3.37	-25.8	-0.50
XI-3	20.0	0.03	0.04	-	0.19	0.18	3.10	-33.2	1.09
XI-4	30.0	0.08	0.09	0.5	0.29	0.28	3.14	-31.2	0.65
XI-5	38.0	0.27	0.27	0.5	0.41	0.39	3.29	-27.2	-0.20
XI-6	20.0	0.04	0.04	-	0.19	0.18	3.06	-34.3	1.36
XII-1	72.0	0.02	0.02	-	0.28	0.28	6.11	-52.0	1.05
XII-2	90.0	0.45	0.58	1.0	0.41	0.38	6.03	-48.2	0.17
XII-3	51.0	-	-	-	0.19	0.18	6.15	-64.0	1.72
XII-4	69.0	0.01	0.01	-	0.29	0.28	6.11	-58.0	1.30
XII-5	90.0	0.28	0.30	0.5	0.41	0.39	6.03	-52.1	0.47
XII-6	51.0	-	-	-	0.19	0.18	6.15	-64.0	1.94

1 in = 25.4 mm

Table 9. (Continued)

RUN NUMBER	MAXIMUM STEERING WHEEL RATE	FRONT WHEEL			MAXIMUM LATERAL ACCEL.	STEADY STATE			
		STEER OVERSHOOT	MAXIMUM OSCILLATION AMPLITUDE	NO. CYLCES TO DAMP		LATERAL ACCEL.	FR WHEEL STEER ANGLE	RR WHEEL OFFSET	BODY SLIP ANGLE
	DEG/SEC	DEG	DEG	-	G's	G's	DEG	IN	DEG
XIII-1	184.0	1.13	1.41	1.5	0.34	0.27	2.52		-0.27
XIII-2	258.0	2.13	3.32	2.0	0.52	0.38	2.61	-23.1	-1.21
XIII-3	118.0	0.41	0.49	1.0	0.20	0.18	2.45	-29.1	0.51
XIII-4	184.0	1.10	1.38	1.5	0.33	0.28	2.48	-27.4	0.05
XIII-5	258.0	2.09	3.12	2.0	0.51	0.38	2.56	-24.2	-0.88
XIII-6	126.0	0.39	0.47	1.0	0.20	0.18	2.41	-30.0	0.80
XIV-1	168.0	0.82	0.99	1.5	0.32	0.28	3.18	-30.0	0.38
XIV-2	220.0	1.83	2.43	1.5	0.49	0.38	3.34	-26.0	-0.48
XIV-3	112.0	0.17	0.24	1.5	0.19	0.18	3.09	-33.2	1.10
XIV-4	166.0	0.78	0.99	1.5	0.32	0.28	3.14	-31.2	0.67
XIV-5	220.0	1.73	2.39	1.5	0.49	0.38	3.29	-27.7	-0.16
XIV-6	112.0	0.18	0.25	1.5	0.19	0.18	3.06	-34.3	1.36
XV-1	198.0	0.19	0.26	1.0	0.31	0.28	6.10	-56.5	1.06
XV-2	267.0	0.75	1.53	1.5	0.48	0.38	6.08	-48.0	0.17
XV-3	138.0	-	-	-	0.18	0.18	6.14	-62.0	1.73
XV-4	198.0	0.10	0.19	1.0	0.31	0.28	6.11	-58.0	1.31
XV-5	270.0	0.48	0.89	1.5	0.48	0.39	6.08	-52.0	0.47
XV-6	141.0	-	-	-	0.19	0.18	6.14	-63.5	1.94

1 in = 25.4 mm

Table 9. (Continued)

RUN NUMBER	FRONT WHEEL				STEADY STATE			
	MAXIMUM STEERING WHEEL RATE	STEER OVERSHOOT	MAXIMUM OSCILLATION AMPLITUDE	NO. CYCLES TO DAMP	MAXIMUM LATERAL ACCEL.	LATERAL ACCEL.	FR WHEEL STEER ANGLE	RR WHEEL OFFSET	BODY SLIP ANGLE
	DEG/SEC	DEG	DEG	-	G's	G's	DEG	IN	DEG
XVI-1	90.0	0.59	0.71	1.0	0.31	0.28	2.53	-26.3	-0.30
XVI-2	132.0	1.15	1.64	1.5	0.46	0.38	2.61	-23.0	-1.25
XVI-3	62.0	0.21	0.22	0.5	0.19	0.18	2.45	-29.0	0.49
XVI-4	90.0	0.54	0.64	1.0	0.31	0.28	2.48	-27.3	0.01
XVI-5	130.0	1.06	1.44	1.5	0.46	0.39	2.56	-24.0	-0.91
XVI-6	60.0	0.18	0.20	0.5	0.19	0.18	2.41	-30.0	0.77
XVII-1	84.0	0.40	0.44	0.5	0.30	0.28	3.19	-29.8	0.36
XVII-2	118.0	0.92	1.12	1.5	0.44	0.38	3.37	-25.7	-0.51
XVII-3	56.0	0.10	0.11	0.5	0.19	0.18	3.10		1.09
XVII-4	80.0	0.38	0.42	0.5	0.30	0.28	3.14	-31.2	0.64
XVII-5	116.0	0.87	1.06	1.5	0.45	0.39	3.28	-27.3	-0.20
XVII-6	56.0	0.09	0.09	0.5	0.19	0.18	3.06		1.35
XVIII-1	102.0	0.07	0.07	0.5	0.29	0.28	6.13	-57.0	1.04
XVIII-2*	138.0	0.57	0.68	1.0	0.43	0.38	5.95		0.19
XVIII-3	72.0	-	-	-	0.19	0.18	6.15		1.73
XVIII-4	102.0	0.05	0.05	0.5	0.30	0.29	6.14	-57.0	1.31
XVIII-5*	138.0	0.46	0.50	0.5	0.44	0.39	5.96		0.49
XVIII-6	72.0	0.01	-	-	0.19	0.18	6.15		1.95

1 in = 25.4 mm

*SIMULATED TIME EXPIRED BEFORE STEADY STATE ACHIEVED. STEADY STATE VALUES ESTIMATED.

Table 9. (Continued)

RUN NUMBER	MAXIMUM STEERING WHEEL RATE	FRONT WHEEL			MAXIMUM LATERAL ACCEL,	STEADY STATE			
		STEER OVERSHOOT	MAXIMUM OSCILLATION AMPLITUDE	NO. CYLCES TO DAMP		LATERAL ACCEL.	FR WHEEL STEER ANGLE	RR WHEEL OFFSET	BODY SLIP ANGLE
	DEG/SEC	DEG	DEG	-	G's	G's	DEG	IN	DEG
XXII-1	144.0	1.38	2.19	3.5	0,34	0.25	0.93	-24.6	-0.86
XXII-2	204.0	2.20	4.16	3.5	0.51	0.34	1.01	-22.0	-1.71
XXII-3	88.0	0.76	1,03	2.5	0.20	0.16	0.86	-27.1	-0.18
XXII-4	142.0	1.38	2.15	3,5	0.34	0.25	0.89	-25.6	-0.54
XXII-5	202.0	2,20	4.06	2.5	0.52	0.35	0.97	-23.0	-1.38
XXII-6	86.0	0.78	0.99	2.5	0.20	0.16	0.82	-28.0	0.12
XXIII-1	126.0	1.18	1.65	2.5	0.33	0.25	1.13	-26.8	-0.58
XXIII-2	172.0	1.87	2.92	2.5	0.50	0.34	1.28	-23.0	-1.34
XXIII-3	86.0	0.62	0.76	2.0	0.20	0.16	1.05	-29.6	0.05
XXIII-4	124.0	1.16	1.67	2.5	0.33	0.25	1.10	-28.0	-0.30
XXIII-5	168.0	1.87	2.94	2.5	0.51	0.35	1.22	-24.5	-1.04
XXIII-6	76.0	0.62	0.78	2.0	0.20	0.16	1.03	-30.7	0.32
XXIV-1	150.0	0.78	1.00	2.5	0.31	0.25	2.00	-41.0	-0.29
XXIV-2*	198.0	1.62	2.73	2.5	0.50	0.34	2.01	-34.0	-1.03
XXIV-3	96.0	0.14	0.20	2.0	0.19	0.16	2.02	-46.0	0.29
XXIV-4	150.0	0.69	0,91	2.5	0.30	0.25	2.00	-43.3	-0.02
XXIV-5*	207.0	1.50	2.22	2.5	0.50	0.35	2.00	-37.0	-0.73
XXIV-6	102.0	0.08	0.12	2.0	0.18	0.16	2.02	-48.0	0.53

1 in = 25.4 mm

*SIMULATED TIME EXPIRED BEFORE STEADY STATE ACHIEVED. STEADY STATE VALUES ESTIMATED.

Table 9. (Continued)

RUN NUMBER	MAXIMUM STEERING WHEEL RATE	FRONT WHEEL STEER OVERSHOOT	FRONT WHEEL MAXIMUM OSCILLATION AMPLITUDE	FRONT WHEEL NO. CYLCES TO DAMP	MAXIMUM LATERAL ACCEL.	STEADY STATE LATERAL ACCEL.	STEADY STATE FR WHEEL STEER ANGLE	STEADY STATE RR WHEEL OFFSET	STEADY STATE BODY SLIP ANGLE
	DEG/SEC	DEG	DEG	-	G's	G's	DEG	IN	DEG
XXV-1	76.0	0.69	0.73	1.5	0.30	0.25	0.93	-24.6	-0.89
XXV-2	106.0	1.14	1.34	2.5	0.44	0.35	1.03	-21.8	-1.76
XXV-3	48.0	0.38	0.51	1.0	0.18	0.16	0.85	-27.0	-0.18
XXV-4	72.0	0.66	0.70	1.5	0.29	0.25	0.88	-25.6	-0.57
XXV-5	102.0	1.05	1.83	3.0	0.43	0.35	0.99	-22.6	-1.40
XXV-6	46.0	0.35	0.47	1.0	0.18	0.16	0.82	-27.9	0.12
XXVI-1	64.0	0.60	0.79	1.5	0.29	0.25	1.13	-26.7	-0.59
XXVI-2	92.0	0.95	1.39	2.0	0.43	0.35	1.30	-23.1	-1.38
XXVI-3	40.0	0.31	0.37	1.0	0.18	0.16	1.06	-29.7	0.04
XXVI-4	60.0	0.56	0.74	1.5	0.29	0.25	1.09	-28.0	-0.30
XXVI-5	84.0	0.90	1.33	1.5	0.43	0.35	1.23	-24.5	-1.07
XXVI-6	42.0	0.29	0.34	1.0	0.18	0.16	1.03	-30.7	0.31
XXVII-1	78.0	0.48	0.52	0.5	0.28	0.25	1.99		-0.25
XXVII-2*	105.0	0.87	1.23	1.0	0.41	0.35	2.08	-34.8	-1.04
XXVII-3	54.0	0.13	0.13	0.5	0.17	0.16	2.01		0.03
XXVII-4*	75.0	0.43	0.48	2.0	0.28	0.25	1.98		0.01
XXVII-5*	102.0	0.78	1.02	2.0	0.41	0.35	2.07		-0.71
XXVII-6	51.0	0.08	0.08	0.5	0.17	0.16	2.02		0.54

1 in = 25.4 mm

*SIMULATED TIME EXPIRED BEFORE STEADY STATE ACHIEVED. STEADY STATE VALUES ESTIMATED.

It is believed that, since the steering errors associated with the spiral transition for the 10 degree curve are small, the discontinuous behavior of the steer angle as illustrated in Figure 21 results from the above described mechanism. As a result of this problem, runs for the 10 degree spiral transition curve were not considered to be meaningful.

The peak and steady state accelerations given in Table 9 were obtained directly from the HVOSM output and are accelerations of the vehicle sprung mass. These accelerations cannot be interpreted directly in terms of frictional requirements between the tires and road because they are not corrected for vehicle roll angle and roadway superelevation. In order to determine friction requirements, steady state tire side forces and normal forces were tabulated for a number of runs. These results are presented in Table 10 along with the frictional requirement predicted from the equation:

$$e + f = \frac{V^2}{AR}$$

where e = superelevation rate, ft/ft (m/m)

f = side friction factor

V = vehicle speed, mph (km/h)

R = curve radius, ft (m)

A = unit conversion factor: $15\ (\text{mph})^2/\text{ft}$

$127.2\ (\text{km/h})^2/\text{m}$.

As seen in the table, the friction requirements obtained from the HVOSM results for the steady state condition are in no case greater than those predicted from the above equation. This equation therefore appears to be appropriate for establishing the steady state friction requirements for horizontal curves.

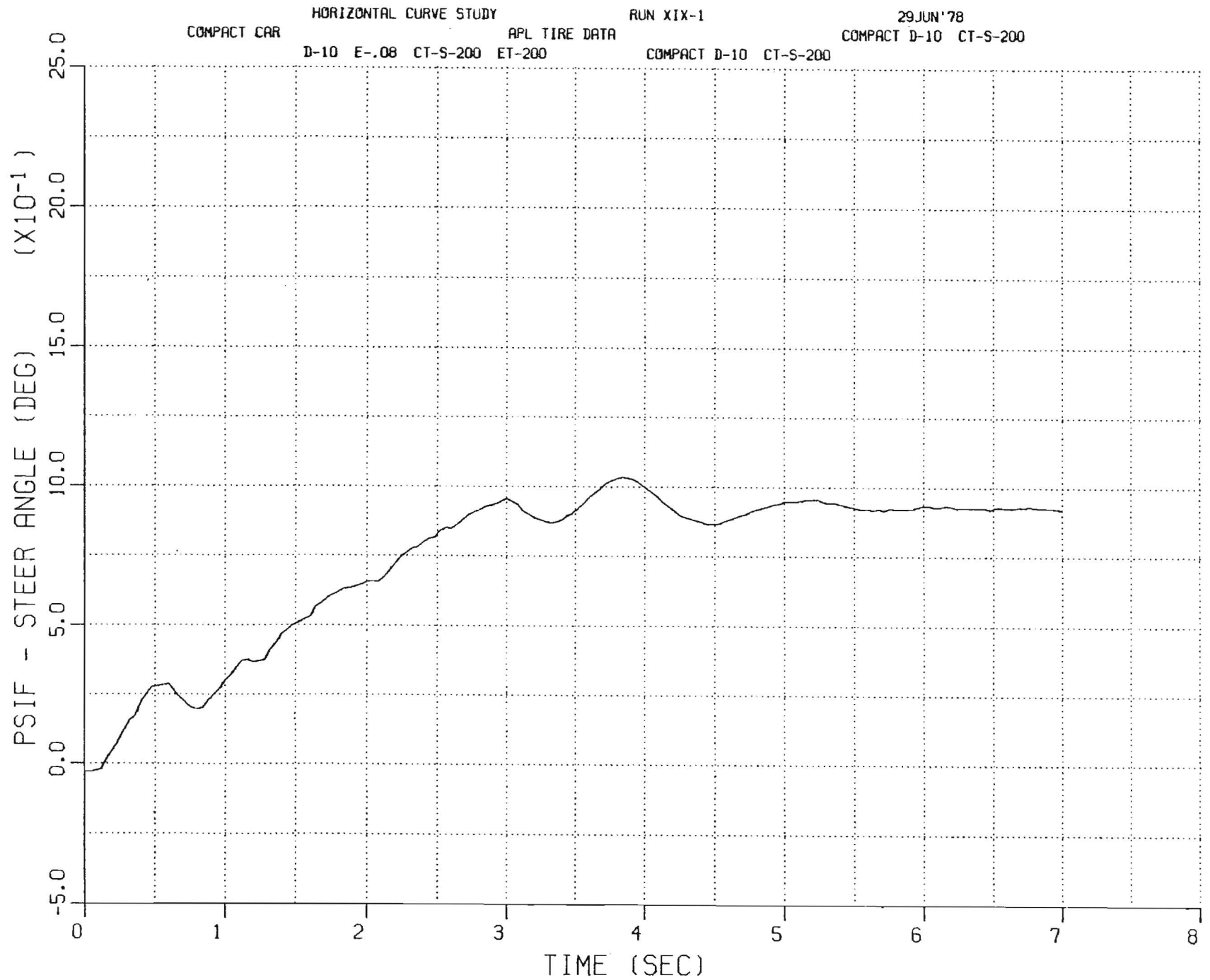

Figure 21. STEER ANGLE FOR 10° SPIRAL TRANSITION CURVE

Table 10. REQUIRED STEADY-STATE SIDE FRICTION FACTORS

RUN NUMBER	VEHICLE	SPEED (MPH)	CURVE	SUPERELEVATION	TOTAL SIDE FORCE (LBS)	TOTAL NORMAL FORCE (LBS)	REQUIRED FRICTION HVOSM	REQUIRED FRICTION PREDICTED
I-1	COMPACT	25.2	36°	.08	554.5	3004.0	.185	.187
I-2	COMPACT	29.7	36°	.08	857.8	3027.3	.283	.290
I-3	COMPACT	20.5	36°	.08	287.0	3001.0	.096	.096
I-4	COMPACT	25.5	36°	.12	449.6	3001.0	.150	.153
II-1	FULL SIZE	25.4	36°	.08	709.5	3793.3	.187	.190
II-4	FULL SIZE	25.6	36°	.12	571.4	3817.6	.150	.154
III-1	SCHOOL BUS	25.4	36°	.08	4533.1	23834.5	.190	.190
III-4	SCHOOL BUS	25.6	36°	.12	3692.8	24105.3	.153	.154
X-1	COMPACT	28.2	30°	.08	581.1	3035.8	.191	.197
X-4	COMPACT	28.3	30°	.12	472.2	3027.2	.156	.160
XXII-1	COMPACT	45.9	10°	.08	489.5	3016.2	.162	.165
XXII-2	COMPACT	46.1	10°	.12	375.4	3037.3	.124	.127

1 mph = 1.609 km/h
1 lb = 4.448 NT

Dynamic vehicle effects, in terms of acceleration response, are illustrated in Table 11 . This table lists the ratio of maximum lateral acceleration to steady-state lateral acceleration, averaged over all vehicles and both superelevation rates, for the three speeds used on each curve. Inspection of these ratios clearly indicates that the type of transition influences the peak acceleration experienced by the vehicle, with the influence becoming more pronounced as the speed around a turn increases. Of particular interest is the fact that a peak acceleration 47% higher than the required steady-state acceleration is obtained for the 10 degree curve with no transition at a speed 20% higher than the design speed.

Table 11. RATIO OF MAXIMUM TO STEADY-STATE LATERAL ACCELERATION (AVERAGED OVER ALL VEHICLES AND SUPERELEVATION RATES FOR EACH SPEED AND TRANSITION)

Curve	Velocity (mph)	Transition		
		Spiral	None	Compound
36°	20.6	1.019	1.029	1.019
	25.7	1.025	1.099	1.049
	30.9	1.053	1.231	1.119
30°	22.9	1.040	1.065	1.056
	28.6	1.030	1.156	1.083
	34.3	1.069	1.297	1.160
10°	37.1		1.219	1.104
	46.4		1.300	1.153
	55.7		1.469	1.214

1 mph = 1.609 km/h

Another view of the acceleration ratio data is given in Table 12 where the peak to steady-state acceleration ratio is listed for each vehicle and curve. The ratios given here are averaged over the three speeds and two superelevations used for each curve. Again, the influence of transition type is obvious, with the difference between peak and steady-state acceleration for the no transition curve averaging approximately 3 to 4 times higher than for the spiral transition curve.

Table 12. RATIO OF MAXIMUM TO STEADY-STATE LATERAL ACCELERATION (AVERAGED OVER ALL SPEEDS AND SUPERELEVATION RATES FOR EACH VEHICLE AND TRANSITION)

		Transition		
Curve	Vehicle	Spiral	None	Compound
36°	Compact	1.030	1.176	1.078
	Full Size	1.039	1.113	1.067
	School Bus	1.027	1.070	1.042
30°	Compact	1.047	1.228	1.119
	Full Size	1.052	1.163	1.094
	School Bus	1.046	1.127	1.057
10°	Compact		1.368	1.183
	Full Size		1.345	1.171
	School Bus		1.276	1.118

Also of interest on this table is the fact that the different vehicles appear to respond differently, in terms of peak dynamic acceleration, to the same curves. This is not unexpected and is due in part to the characteristics of the vehicles themselves and in part due to the automatic guidance systems used. Linear automobile theory, predicts that the compact car is considerably less damped in yaw than the school bus, thus the difference in overshoot, as indicated by the ratio differences is to be expected. The influence that the automatic guidance systems have on this

behavior is not easily defined. Since the point at which steer command errors were calculated was arbitrarily located one wheelbase in front of the front wheel centerline, this longer distance on the school bus may provide more lead time and introduce more effective damping into the system as compared with the compact car.

Table 13 lists the maximum steering wheel angles (steady-state plus overshoot) required by the vehicles for each curve and transition simulated. The values listed are averages of both the 8 and 12 percent superelevation rate runs. As with the acceleration data presented above, the spiral transition appears best, requiring the least total steering angle. Increasing speed on a given curve generally increases steering activity, although this effect is substantially less marked with the school bus than with the automobiles. School bus steering characteristics are further discussed later.

In addition to maximum steering wheel angles required, the maximum steering wheel rates provide some insight into the relative difficulty of traversing the curves studied. These maximum steering wheel rates in degrees/second, averaged for both superelevations, are given in Table 14 . For all vehicles, the maximum rate requirements are substantially less for the spiral transition on the 36° and 30° curves. If the assumption is made that curves should be designed to minimize requirements on the vehicle driver, then the spiral transition shows clear superiority by this measure. However, it should also be pointed out that the maximum rates obtained in this study are well within typical driver capabilities of approximately 500-600 degrees/second (Reference 17). Some difficulty might be encountered in guiding the school bus around the ideal 36° turns, however, since maximum steering wheel angle requirements exceed 180°, which together with rate requirements in excess of 200 degrees/second may require a hand-over-hand steering maneuver on the part of the driver.

Table 13. MAXIMUM STEERING WHEEL ANGLES - DEGREES
(AVERAGED FOR EACH SUPERELEVATION RATE)

CURVE	VELOCITY	SPIRAL TRANSITION			NO TRANSITION			COMPOUND CURVE TRANSITION		
	(MPH)	COMPACT	FULL	BUS	COMPACT	FULL	BUS	COMPACT	FULL	BUS
	20.6	58.4	74.2	222.1	63.0	74.9	221.8	60.7	74.6	222.0
36°	25.7	61.3	77.0	220.9	77.4	86.7	222.3	68.5	81.3	222.4
	30.9	67.0	84.3	226.1	98.1	107.9	234.8	80.1	93.3	227.4
	22.9	49.0	62.3	184.5	56.6	65.0	184.2	52.5	63.5	184.6
30°	28.6	52.6	65.2	183.8	72.3	79.2	187.5	61.4	71.1	185.8
	34.3	57.6	72.7	191.8	93.9	101.2	200.8	73.8	84.4	194.1
	37.1				32.2	33.2	63.9	24.0	26.9	63.6
10°	46.4				45.8	45.7	82.1	31.6	33.8	73.2
	55.7				63.8	62.4	107.0	42.1	43.8	87.0

1 mph = 1.609 km/h

Table 14. MAXIMUM STEERING WHEEL RATES - DEGREES/SECOND (AVERAGED FOR EACH SUPERELEVATION RATE)

CURVE	VELOCITY	SPIRAL TRANSITION			NO TRANSITION			COMPOUND CURVE TRANSITION		
	(MPH)	COMPACT	FULL	BUS	COMPACT	FULL	BUS	COMPACT	FULL	BUS
	20.6	19.2	25.2	69.9	126.0	117.0	141.0	64.0	58.0	76.5
36°	25.7	27.5	33.3	91.1	191.0	169.0	201.0	95.0	84.0	105.0
	30.9	41.4	45.8	119.4	259.0	230.0	276.0	132.0	118.0	142.5
	22.9	16.0	20.0	51.0	122.0	112.0	139.5	61.0	56.0	72.0
30°	28.6	24.0	31.0	70.5	184.0	167.0	198.0	90.0	82.0	102.0
	34.3	35.0	41.0	90.0	258.0	220.0	268.5	131.0	117.0	138.0
	37.1				87.0	81.0	99.0	47.0	41.0	52.5
10°	46.4				143.0	125.0	150.0	74.0	62.0	76.5
	55.7				203.0	170.0	202.5	104.0	88.0	103.5

1 mph = 1.609 km/h

Another indication of the relative difficulty of traversing the curves studied is contained in Figure 22 which illustrates the magnitude of steering overshoot as a percentage of the steady-state steering requirements as a function of speed and transition type. These data are, again, averaged for both superelevation rates considered. Following an ideal no transition curve results in substantial steering overshoot, particularly at the higher speeds. In fact, results for the above design speed 10° no transition curve for the compact vehicle indicate that a counter-steer is necessary to control the vehicle as illustrated in Figure 23

One potentially significant result of this study can be observed by looking at the steer characteristics of the vehicles operating on curves. By plotting the steady-state steer angle against acceleration (in this case V^2/R, the total acceleration of the vehicle) the vehicle understeer factor can be obtained by measuring the slope of a line through the data points. The understeer factor has units of degrees/g and is positive for an understeering vehicle, negative for an oversteering vehicle and zero for a neutral steering vehicle. Such a plot is shown in Figure 24 which is derived from runs using the full size vehicle traversing the 36° curve with spiral transition. Also shown on this figure are the steering characteristics for the same vehicle predicted from linear vehicle dynamics theory and from two HVOSM runs traversing the same curve, but without superelevation.

On the figure, it is seen that linear theory predicts an understeer factor of 0.631 °/g while results from the HVOSM traversing the flat curve indicate an understeer factor of 1.306 °/g. This increase in the understeer factor with the HVOSM is to be expected because the effects of camber change with ride position and tire cornering stiffness change with normal load, both considered in the HVOSM but neglected in the linear theory, constitute understeer effects, that is, they increase a vehicle's understeer factor.

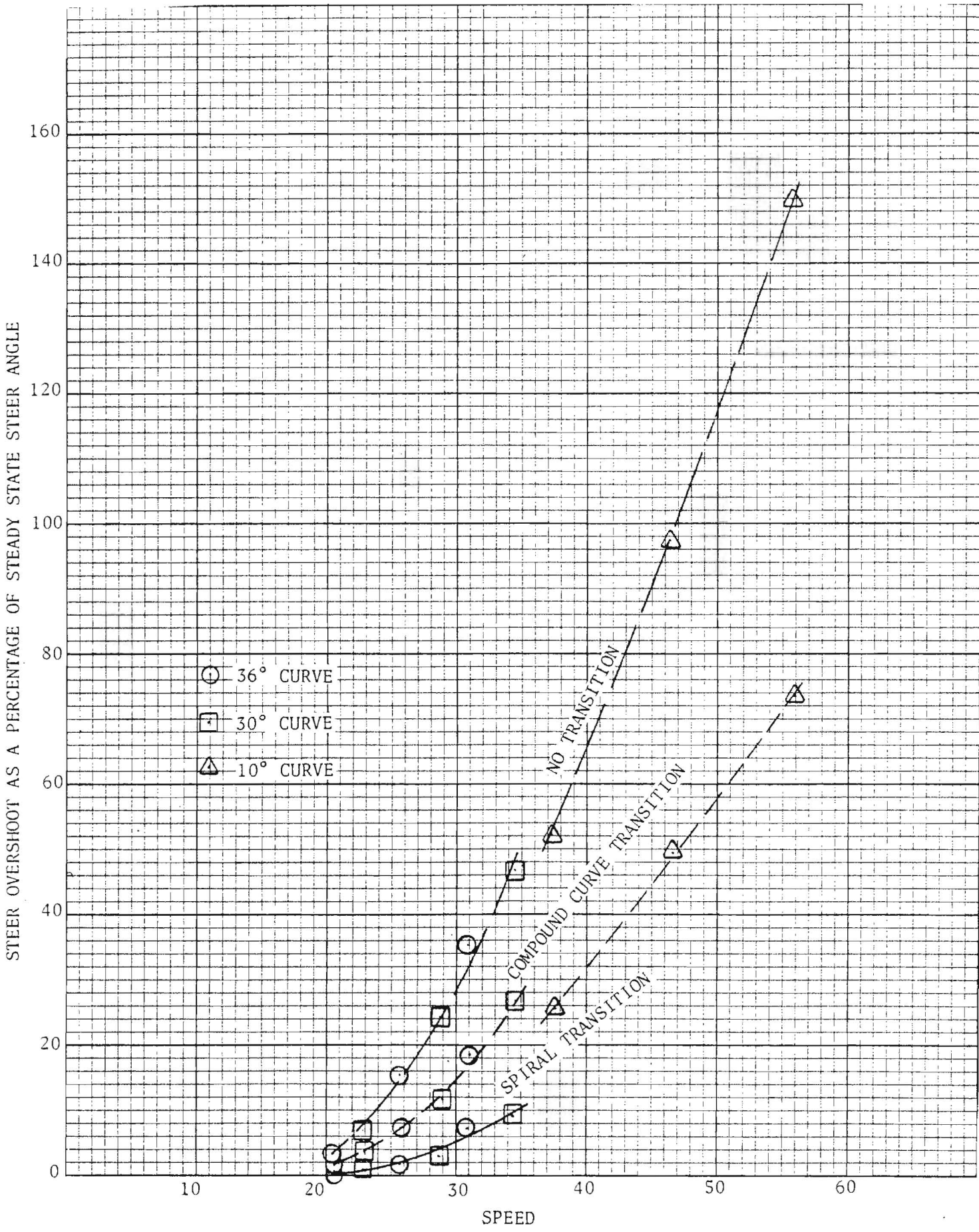

Figure 22. STEERING OVERSHOOT VS. SPEED AND CURVE

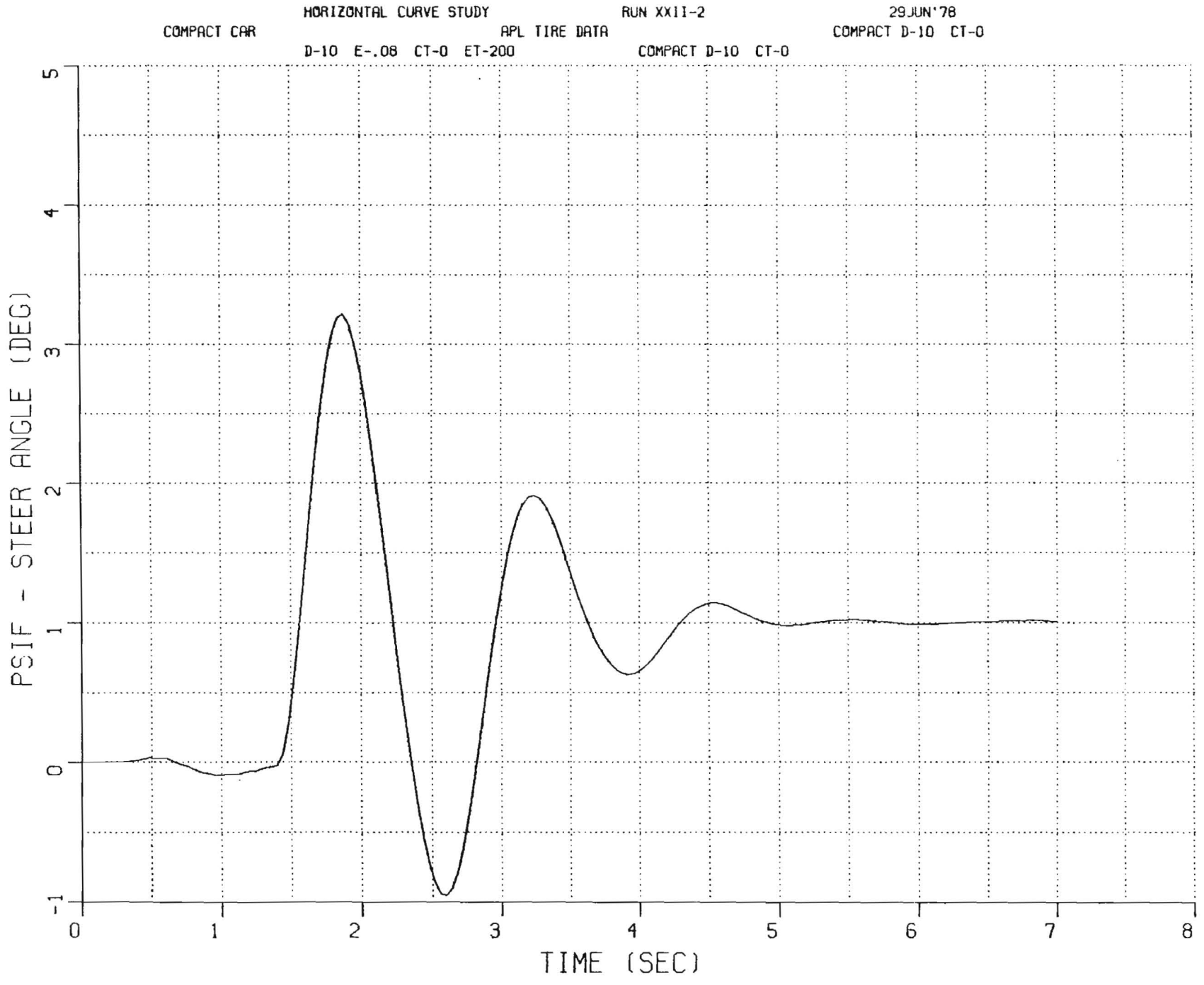

Figure 23. EXAMPLE OF COUNTERSTEER REQUIRED FOR PATH FOLLOWING

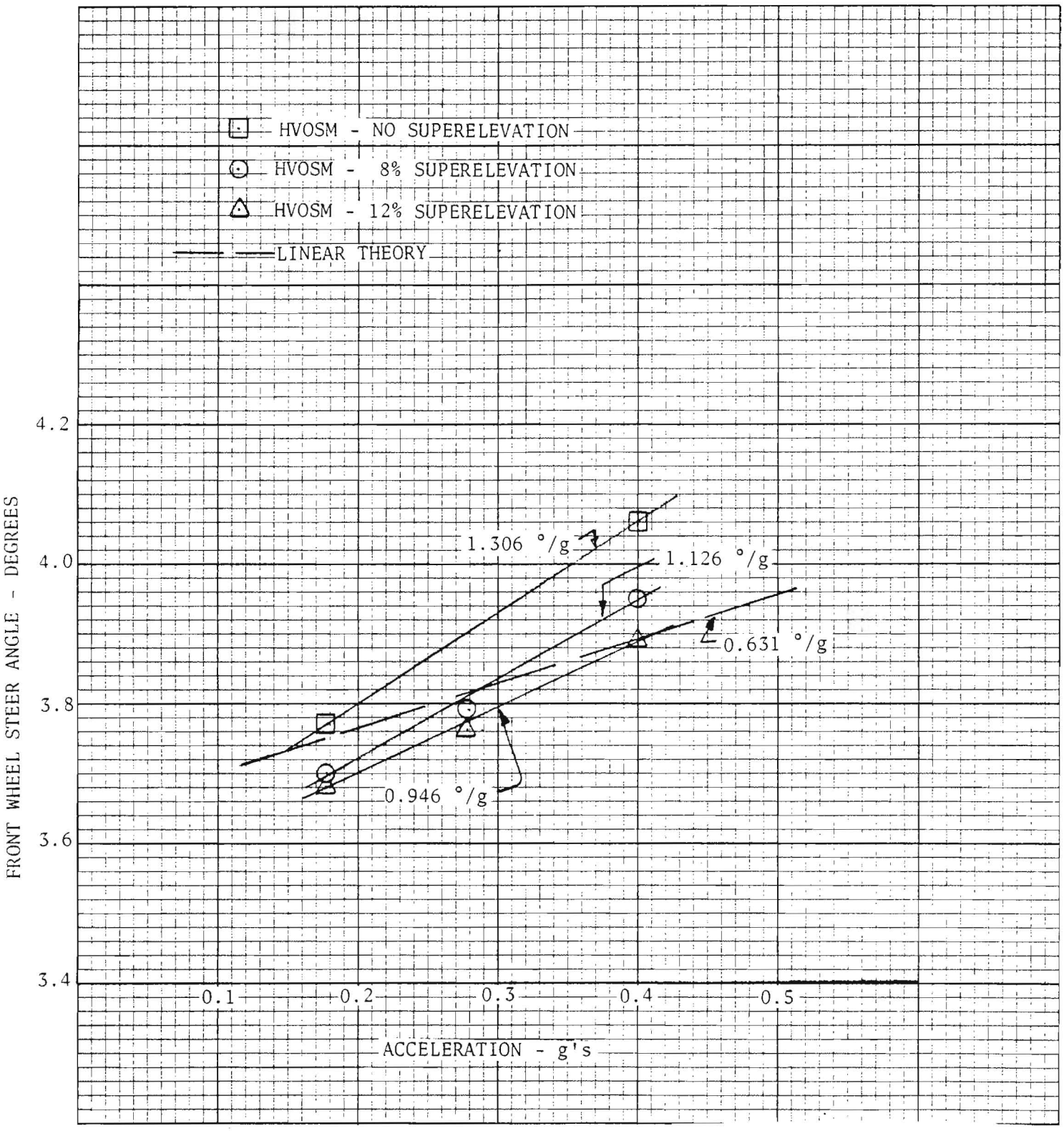

Figure 24. FULL SIZE CAR STEER CHARACTERISTICS

Of particular interest on this figure is, however, that the HVOSM results for the two superelevated curves yield understeer factors of 1.126 and 0.946 °/g for the 8 and 12 percent superelevation rates, respectively. These values reflect a 13.8% and 27.6% decrease in the vehicle's understeer factor when compared with the flat curve HVOSM results. The implication to be drawn from these results is that superelevation changes a vehicle's steer characteristics, and that change is in a direction toward oversteer with the subsequent possibility for instability. Constraints on the study precluded making additional simulation runs to confirm this result with the compact car.

A similar graph of steer angle as a function of lateral acceleration for the school bus is shown in Figure 25 . Simulation results indicate that this vehicle is in an oversteer configuration with an understeer factor of approximately -0.586 °/g. Steer results for the school bus on the other curves also confirm this oversteering behavior. This result was unexpected since linear theory predicts a positive understeer factor of approximately 0.563 °/g. In checking the output of these school bus runs in some detail, it appears that the front tires consistently developed more side force than they apparently should have under the operating conditions of slip angle and normal load. Sufficient output was not available to determine whether camber properties of these tires resulted in this excessive side force and limitations on time and funding precluded an in-depth investigation to establish the cause. It is therefore not currently known whether this behavior results from an anomaly in the tire data or a deficiency in the tire model under these operating conditions.

The right wheel offset from the ideal path results contained in Table 9 indicate that, as would be expected, the automobiles exhibit no problem with tracking off the pavement on any of the curves. However, the school bus, with its 245 inch (6.0 m) wheelbase tracks with its right rear tire about 68 inches (1.73 m) from the centerline of the 36° curve. Thus, even under the ideal conditions of perfect tracking of the lane centerline, the bus comes within four inches of leaving a 12 foot (3.66 m) wide lane.

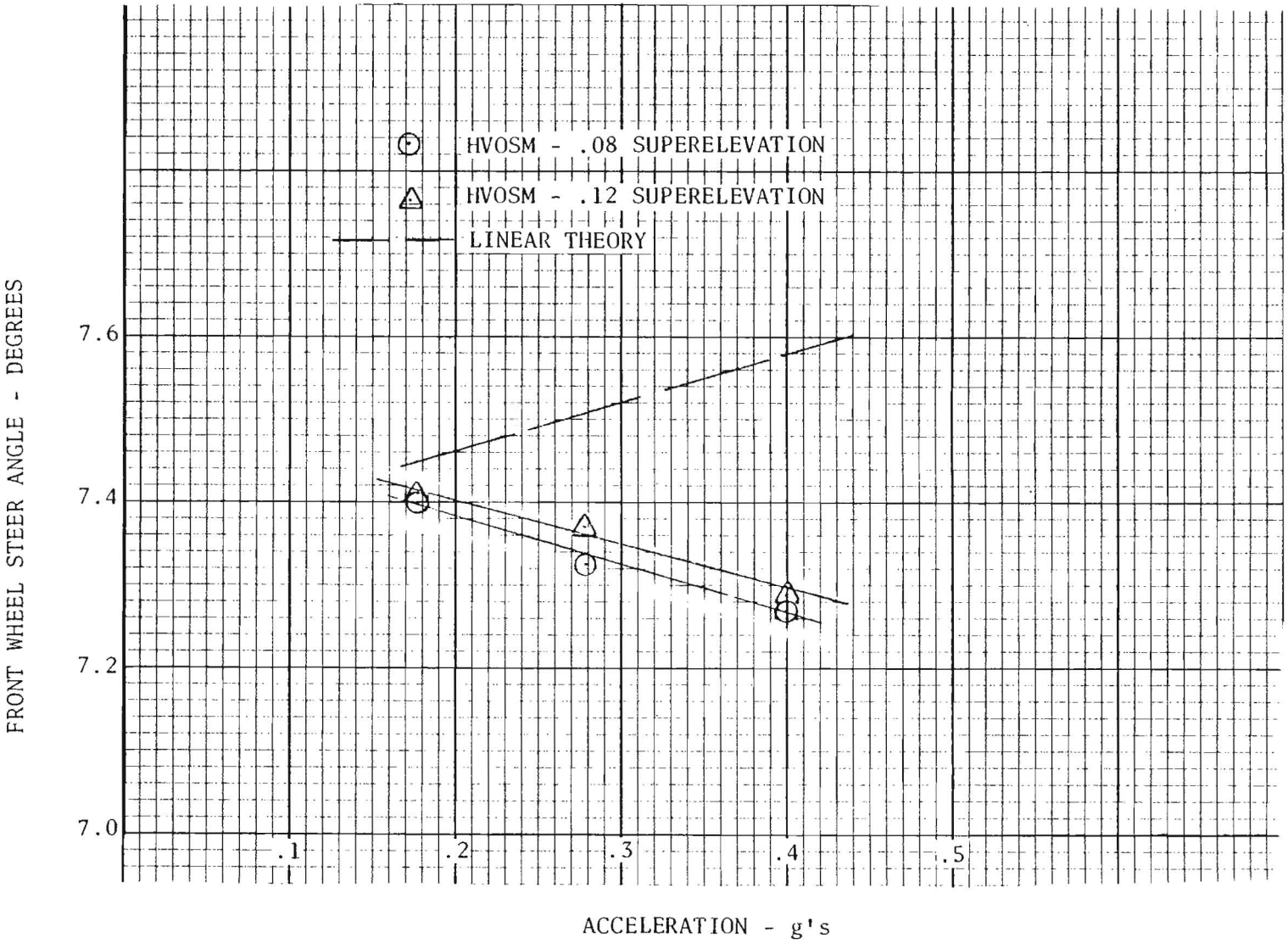

Figure 25 SCHOOL BUS STEER CHARACTERISTICS

4. CONCLUSIONS AND RECOMMENDATIONS

4.1 Conclusions

1. Based upon the analysis of observational data for three curves, it can be concluded that on the two sharp curves (31° and 38°), the heavier vehicles (school buses and tractor-trailers) used more of the roadway for negotiation of the entrance transition than did automobiles. For both curves, the majority of the observed tractor-trailers selected paths involved departure from the road and use of the shoulder. This phenomenon is not related only to the degree of curvature since it was observed that the proportion of vehicles departing the roadway was greater for the 31° curve than for the 38° curve.

2. The mean speeds of the observed vehicles traversing the three curves were not, in all cases, consistent with the AASHTO recommended design speeds. For the 38° curve the recommended design speed is approximately 23 mph (37.0 km/h) while the mean observed speeds were about 27 mph (43.4 km/h) for the automobiles and about 23 mph (37.0 km/h) for the school buses and tractor-trailer. For the 31° curve, the recommended speed is about 27 mph (43.4 km/h) and the observed speeds were approximately 28 mph (47.8 km/h), 27 mph (43.4 km/h) and 24 mph (38.6 km/h) for the automobiles, school buses and tractor-trailers, respectively. The recommended design speed for the 8° curve is approximately 47 mph (75.6 km/h) while the mean travel speeds were about 43 mph (69.2 km/h), 39 mph (62.8 km/h) and 41 mph (66.0 km/h) for the automobiles, school buses and tractor-trailers.

3. Based upon the analysis of mean path data for three vehicle types (auto, school bus, tractor-trailer) through three curves, it can be concluded that the negotiation of an entrance transition can be characterized as consisting of three phases: a preparation, a transition, and curve following. The preparation is a move away from the curve direction which positions the vehicle in the center of the travel lane. This allows for the selection of a transition path which is somewhat less demanding than the path of the given curve. The transition starts approximately 40 feet (12.2 m) before the PC and involves a change in direction in which the vehicle moves in the direction of the curve. Depending upon the path selected, the transition consists of a number of successive path revisions leading to a path which follows the curve.

   Comparison of the mean paths with individual paths reveals that most paths include a preparation and transition, but very few vehicles ever stabilize into a path which follows the curve. The curve following phase may therefore be an artifact of the mean path. The analysis questioned the use of mean paths as being representative of how drivers negotiate curves.

4. No articulated vehicle simulations are available that combine the necessary features for simulating lateral vehicle dynamics coupled with variable terrain associated with superelevated curves.

5. The HVOSM provides a useful tool for simulating non-articulated vehicles traversing superelevated curves. However, a question regarding the validity of the tire model for simulating truck tires remains in that the HVOSM did not produce the steer response characteristics of the school bus that were expected.

6. The current AASHTO horizontal curve design results in a good prediction of steady-state side friction factor requirements based on comparison with the calculated tire side and normal forces output from the HVOSM.

7. The transition from tangent section to circular curve results in transient vehicle dynamics that can substantially increase friction requirements over the steady-state value. The transient vehicle lateral acceleration was found under the conditions simulated to be as much as 50% greater than the steady-state acceleration for the no transition curve. The lateral acceleration transient overshoot for the spiral transitions simulated was less than 10% of the steady-state value.

8. Perfect tracking around a horizontal curve with no transition imposes greater requirements on the driver, in terms of maximum steering wheel angles and rates required, and greater requirements on maximum side friction factor. It must be recalled that the driver model employed in this study was an idealized one and that real drivers will effect their own transition. The simulation results for the no transition curve should therefore be regarded as a worst case condition in the interval where steering transition occurs. It can be concluded that a spiral transition allows easier following of the ideal path than either the no-transition or compound-transition curves.

9. Vehicle speed plays a most significant role in dynamics of a vehicle both in a relative sense (i.e., the speed at which a given curve is traversed) and in an absolute sense (the design speed of a curve). As vehicle speed increases, vehicle yaw damping decreases, thus resulting in a more oscillatory system. As a result, increasing speed on a given curve increases acceleration and steering overshoot while increasing curve design speed also increases overshoot and the number of steering cycles required to damp the system. A

preliminary implication drawn from the results of this study suggest that close attention be paid to transitions for high speed curves since, at high speed, the vehicle itself tends to be more oscillatory,

10. Long wheelbase vehicles must be expected to have difficulty remaining within a 12 foot (3.7 m) lane on a small radius curve (e.g., 36°). Even with perfect tracking of the lane centerline the school bus right rear tire comes within 4 inches (102 mm) of leaving the lane. It therefore must be expected that a significant percentage of such vehicles would negotiate such a curve with at least one tire on the shoulder.

11. Superelevation does not appear to play a significant role in effecting transient vehicle dynamics on curves, at least as indicated by the measures used. However, it does appear that superelevation influences the steady-state steer characteristics of vehicles. The tendency indicated from the simulation results is that increasing superelevation decreases a vehicle's understeer factor. This observation may be significant in that a driver may not anticipate such handling differences and may therefore apply more steering that is required leading to the need for successive steering corrections in order to maintain path.

12. The transition length recommendations for compound curve transitions are substantially higher than those for a spiral transition into the same degree of curve. This does not appear to be warranted based on lateral dynamics of the vehicle.

4.2 Recommendations

1. Based on the results obtained from the simulation study, it is recommended that spiral transitions be used to the greatest extent possible in highway construction.

2. An existing articulated vehicle simulation should be modified so that superelevated curves can be considered in subsequent studies. If superelevation does in fact result in changes to steer characteristics, this effect may be more significant with articulated vehicles than with conventional vehicles.

3. Additional effort should be applied toward confirmation of the change in steady-state steer characteristics on superelevated curves. The change in the full size car understeer factor toward less understeer should be confirmed with the analysis of results of other vehicles traversing superelevated curves. In addition, the tire model and data used in the school bus simulations should be further investigated in order to establish the cause of the apparently anomalous steering behavior.

4. If further studies of heavy vehicles are to be made with the HVOSM, a more rigorous model of dual rear tires should be considered. Such a modification would involve simulating each of the four tires on a dual wheel axle independently.

5. A methodology for relating simulation results to observational behavior should be established. Since observational data only became available late in the present study, sufficient time was not available to make significant progress toward this goal. However, results indicate that it may be necessary to consider data collection at closer intervals in order to extract meaningful steer behavior from the observed vehicle trajectories.

6. Roadway design criteria should take into account not only steady-state lateral acceleration (or required side friction factor) but the expected maximum transient acceleration. More research is required in order to establish this expected maximum as a function of curve geometrics.

7. The results of this study indicate a possible interaction between path selection and velocity. It is recommended that any further attempt to characterize vehicle paths through curves should consider this interaction. One possibility would be to stratify the subject vehicles according to the approach velocity and consider differences in selected path as a function of velocity. In this way, the mean path may be found to be more representative of the individual paths within these groups.

8. Because the three curves used in the observational study differ in so many ways, it was not possible to determine the reasons for differences in paths. It is therefore recommended that in order to determine the critical determinants of path selection, a more systematic study be undertaken in which curves are selected to allow the attribution of differences to specific roadway or operational features. In addition, the study should include left curves as well as right curves.

9. Because in the current analysis the representativeness of the mean paths was questioned, it is recommended that further analysis of this type consider alternate measures of central tendency such as modal paths.

5. REFERENCES

1. Segal, D. J., "Highway-Vehicle-Object Simulation Model - 1976," Report No. FHWA-RD-76-162 through 165, February 1976.

2. Glennon, J. C. and Weaver, G. D., "Highway Curve Design for Safe Vehicle Operations," Highway Research Board, Highway Research Record #390, 1972.

3. Segal, D. J., "Automatic Guidance of Pneumatic Tired Vehicles," Calspan Internal Research Report No. YC-2810-V-1, October 1972.

4. Fancher, P. S., et al, "Limit Handling Performance as Influenced by Degradation of Steering and Suspension Systems, Highway Safety Research Institute Report No. UM-HSRI-PF-72-3-1, November 1972.

5. Correspondence from Mr. A. L. Schnieg, Chief, Highway Safety Division, Bureau of Surface Trnasportation Safety, National Transportation Safety Board.

6. Ervin, R. D., et al, "Effects of Tire Properties on Truck and Bus Handling, Volumes I-IV," Highway Safety Research Institute, PB-263878 through 881, December 1976.

7. Weir, D. H., et al, "Analaysis of Truck and Bus Handling, Volume II," Systems Technology, Inc., PB234197, June 1974.

8. A Policy on Geometric Design of Rural Highways, American Association of State Highway Officials, 1965.

9. Hales, F. D., "The Lateral Stability of a Simplified Articulated Vehicle," The Institution of Mechanical Engineers publication, London, 1963.

10. Hales, F. D., et al, "The Handling and Stability of Motor Vehicles, Part 3, The Lateral Stability of Articulated Vehicles under Braking Conditions," The MIRA Report No. 1966/3, 1966.

11. Bundorf, T. R., "Directional Control Dynamics of Automobile-Travel Trailer Combinations," SAE Paper 670099, 1967.

12. Krauter, A. I. and Wilson, R. K., "Simulation of Tractor-Semitrailer Handling," SAE Paper 720922, 1972.

13. Eshleman, R. L., et al, "Stability and Handling Criteria of Articulated Vehicles, IIT Research Institute, PB-225021/5, September 1973.

14. Johnston, D. E., et al, "Handling Test Procedures for Passenger Cars Pulling Trailers, Volume II - Technical Report," Systems Technology Inc., PB-256072, June 1976.

15. Bernard, J. E., et al, "A Computer Based Mathematical Method for Predicting the Directional Response of Trucks and Tractor-Trailers, Phase III Technical Report," Highway Safety Research Institute, PB-221630, June 1973.

16. Snelgrove, F. B., "Articulated Vehicle Research in Ontario, Proceedings of a Symposium on Commercial Vehicle Braking and Handling, Highway Safety Research Institute, May 1975.

17. Rice, R. S. and Dell'Amico, F., "An Experimental Study of Automobile Driver Characteristics and Capabilities," Calspan Report, No. ZS-5208-K-1.

APPENDIX A

OBSERVATIONAL DATA COLLECTION METHODOLOGY

Selection of Observational Sites

The selection of horizontal curves for use as observational sites involved the evaluation of candidate curves based upon the following criteria:

a) Degree of curvature of approximately 10°, 30°, or 36°

b) Minimal grade change through curve

c) Approach along a tangent section

d) Minimal opportunity for disruption of traffic flow due to conflicting traffic such as from intersection, or prominent roadside features such as shopping centers

e) ADT level such that the curves are used regularly by automobiles, tractor-trailers, and school buses in a free flow situation

f) Curve must allow opportunity for experimental vehicle to enter traffic stream behind subject vehicles.

In order to find a 30° or 36° curve which is used regularly by both school buses and tractor-trailers, it was necessary to consider entrance and exit ramps associated with limited access roads. It was determined that the only other existing curves of this curvature would be on narrow roads of relatively poor quality, which are rarely used by tractor-trailers.

Prior to the selection of curves for the study, numerous curves were observed for the purpose of locating school bus and tractor-trailer traffic. In addition, local school bus dispatchers were contacted in order to determine routes and schedules of school buses on various candidate curves.

The curves selected for use in the study are shown schematically in Figures 26 through 28, and the curve geometrics, as called out on the construction drawings, are given in Table 15 .

The 38° curve shown in Figure 26 is at the end of an exit ramp from the westbound lane of a limited access highway to the southbound lane of a local route. This curve was used regularly by all of the required traffic types, and heavily during rush hours. It had no designed-in transition between tangent and circular segments and was essentially flat with very little superelevation. The chase vehicle was stationed at the location marked by (1) on the figure in order to intercept and follow the vehicles being observed.

A schematic diagram of the 31° curve is shown in Figure 27 . This curve is on an entrance ramp from a local highway northbound to a limited access highway westbound. The traffic mix and patterns for this curve were essentially identical to those seen on the 38° curve; however, it differed in that it contained a slight upgrade and had a substantial superelevation. This curve also had no designed-in transition. The chase vehicle was stationed at the location indicated as (1) on the figure to await the desired experimental vehicles.

The 8° curve studied is shown schematically in Figure 28 . This curve is part of an entrance ramp to a limited access highway eastbound from a parallel local route. The approach to the curve is along a two-lane tangent section of the ramp. As indicated in the geometrics shown in Table 15 , a designed-in 150 ft. (45.7 m) spiral provided a transition between the tangent and circular curve. The chase vehicle was stationed along the tangent for intercepting and following the observed vehicles.

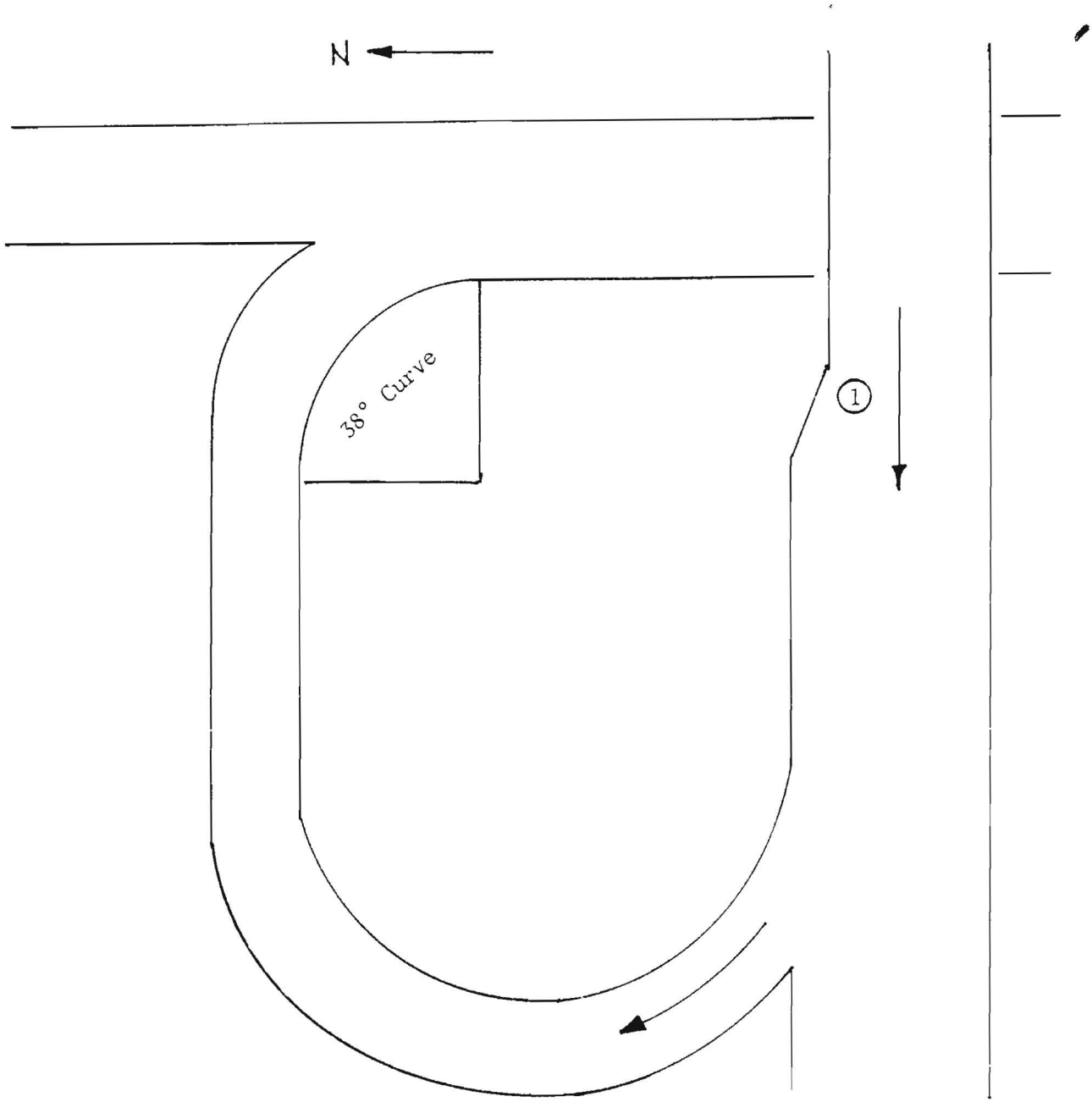

Figure 26. SCHEMATIC DIAGRAM OF 38° CURVE

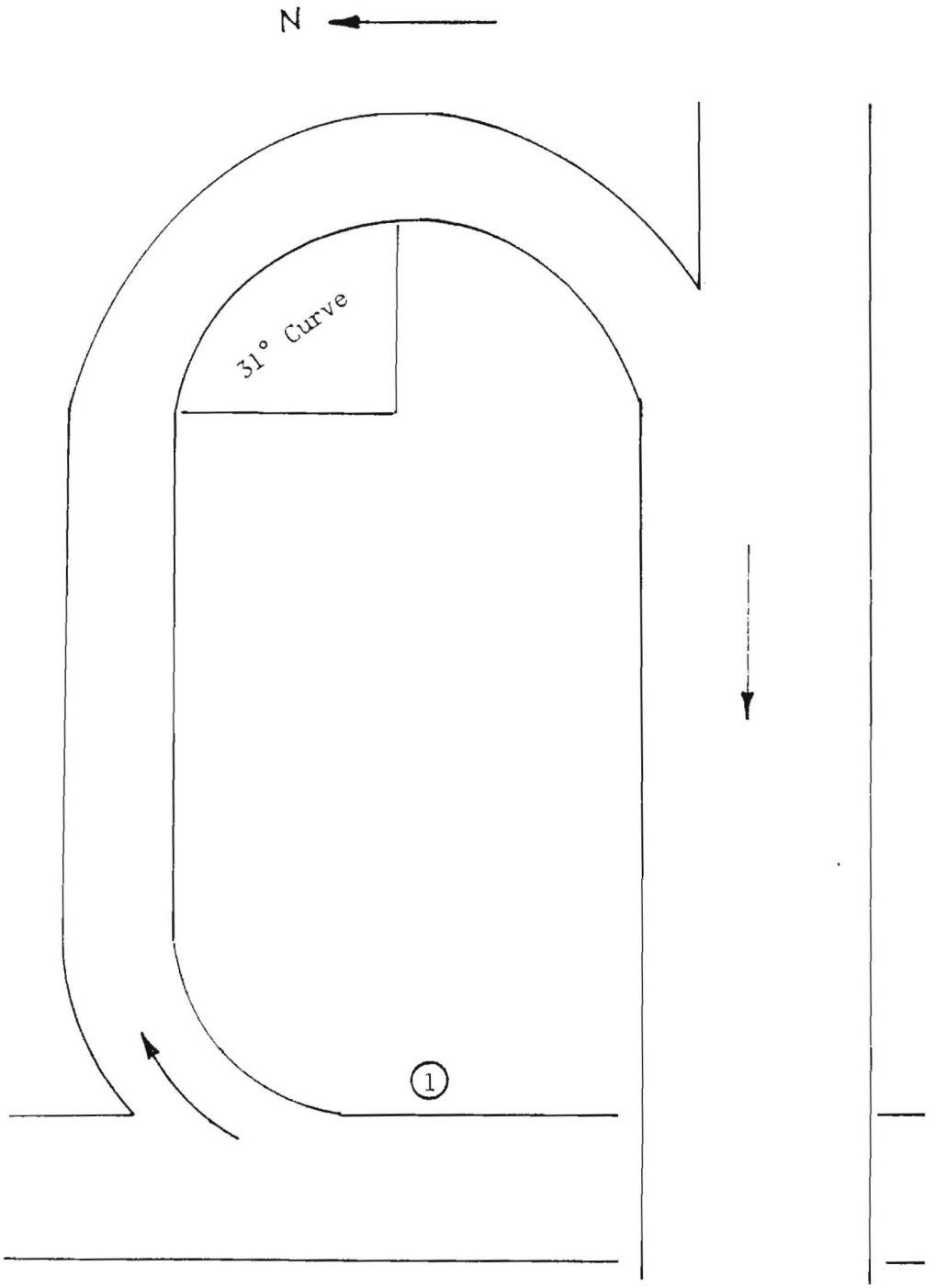

Figure 27. SCHEMATIC DIAGRAM OF 31° CURVE

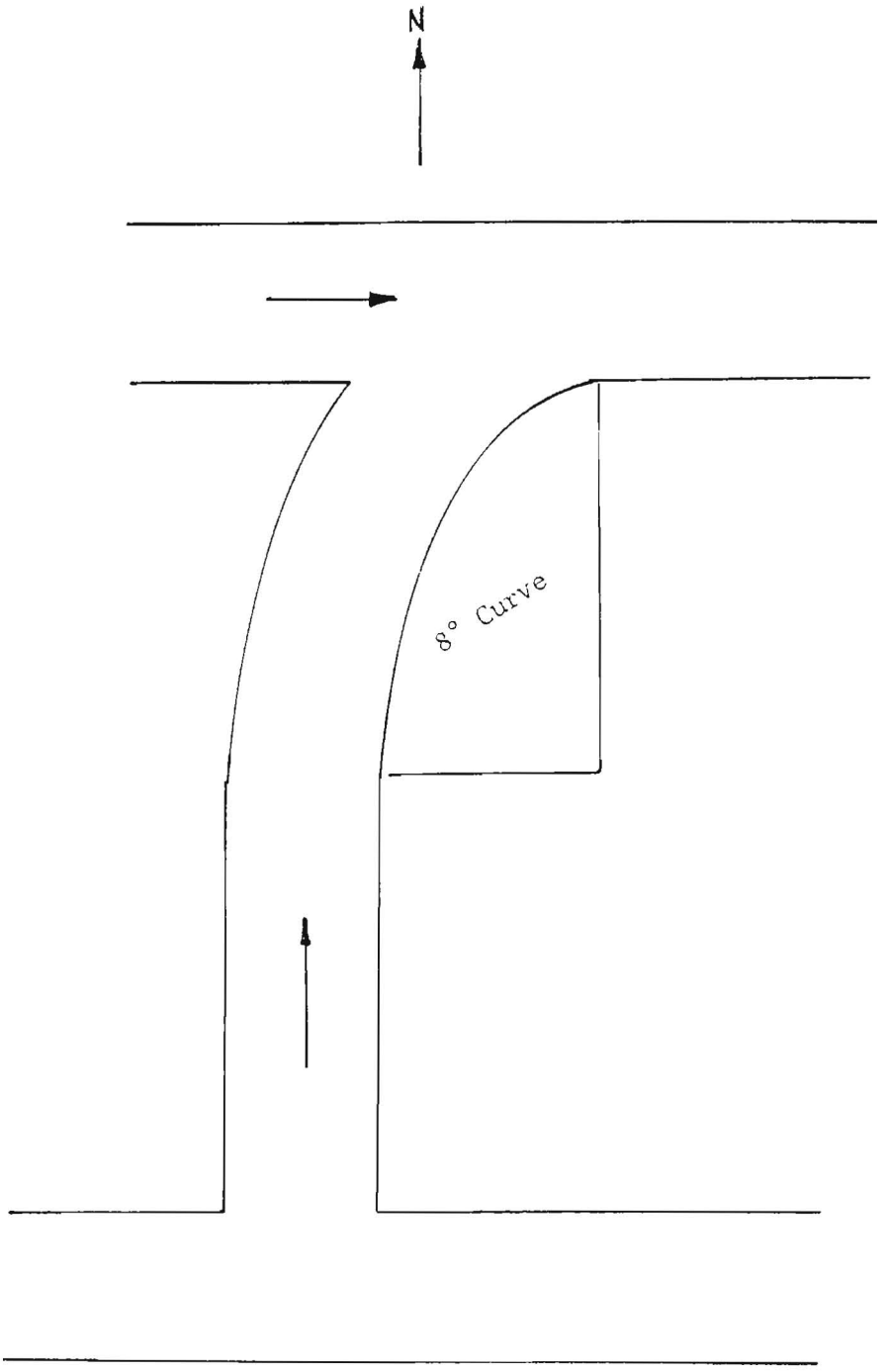

Figure 28. SCHEMATIC DIAGRAM OF 8° CURVE

Table 15. CURVE GEOMETRICS

Curve Descriptors		38° Curve	31° Curve	8° Curve
Angle of Intersection	I (degrees)	90.00	117.47	94.51
Radius	R (feet)	150.00	180.00	716.20
Degree of Curve	D (degrees)	38.20	31.83	8.00
Tangent	T (feet)	150.00	247.05	
Length of Curve	L (feet)	235.62	369.05	1031.42
Center Angle of Spiral	Δ (degrees)			6.00
Tangent of Spiraled Curve	T_S (feet)			851.35
Length of Spiral	L_S (feet)			150.00

1 foot = 0.305 m

Preparation of Observational Sites

For each of the selected curves, a distance interval for data collection was defined that included a road segment in which drivers were required to make the transition from a straight road to the circular curve. The 31° and 38° curves were divided into three 100 foot (30.5 m) segments, one before and two following the point of curvature (PC). This was based upon the observation that virtually all vehicles had completed the transition from straight to curve at PC +200 feet (61 m). These intervals were used for the collection of velocity data. Each of these intervals was further divided into 20 foot (6.1 m) intervals at which measurement of the subject vehicle's lateral position was made. Because neither the 31° or 38° curve involved a built-in transition, the data collection interval included 100 feet (30.5 m) of tangent and 200 feet (61.0 m) of curve. For these two curves, the PC was located visually by inspection of the road.

For the 8° curve, since vehicles traveled at higher speeds and because the curve was longer, it was decided to collect data over a total distance of 480 feet (146.3 m) consisting of three 160 foot (48.8 m) intervals. The first interval included approximately 70 feet (21.3 m) of tangent and 90 feet (27.4 m) of the spiral transition. The second interval included the remainder of the spiral transition and 100 feet (30.5 m) of circular curve. The third 160 foot (48.8 m) segment was entirely on the circular curve. The existence of the spiral transition curve made it extremely difficult to locate the PC visually. The PC was therefore located through calculation of distance from a fixed reference point on the construction drawing. Vehicle lateral position measurements were obtained at 40 ft. (12.2 m) increments along the roadway.

The roadway markings consisted of 24 x 6 inch (610 x 152 mm) white lines painted perpendicular to the right edge of the road. For easy identification of the specific location on the film,* a pattern of crosses was used at certain

*See following discussion of data collection procedures.

intervals. Each of the larger intervals were marked with two lines on the right and one on the left.*

For each of the marked points along each of the selected curves, the superelevation was measured. The values are presented in Table 16 .

Collection of Observational Data

Observational data included path and velocity data. Path data were collected photographically from the experimental vehicle which followed the subject vehicles through the three curves. The experimental vehicle was manned with a photographer and driver. The photographer was seated in the front passenger seat of the vehicle. Using a 35 mm SLR camera attached to a battery-operated motor drive, the photographer shot a continuous sequence of pictures for each subject vehicle. The camera was set to operate at either 2.5, 3 or 3.5** frames per second depending upon the approximate speed of the subject vehicle. Film canisters loaded with approximately 40 feet (12.2 m) of black and white film allowed approximately 15 vehicles per canister. The intention was to ensure that a frame associated with each of the roadway divisions was obtained.

---

* This arrangement was adopted following extensive experimentation with different color paints, ones which were likely to be less visible to the drivers of the subject vehicles. However, at certain times of day, and in certain weather conditions, the less visible lines were not visible on the film. It was decided that, in order to ensure the existence of readable markers on the film, white paint would be used. Several Calspan employees known to regularly use one of the selected curves were found to be unaware of the painted markings, indicating that the markings were not necessarily noted by the subject drivers.

** Following Glennon and Weaver (Reference 2), it was originally intended that a constant rate of the motorized camera would allow a calculation of velocity. However, it was determined that the speed of the camera was variable and, therefore, not reliable for use in calculation of velocity.

Table 16.

CURVE SUPERELEVATION RATES

Position (feet)	38° Curve Superelevation-%	31° Curve Superelevation-%	Position (feet)	8° Curve Superelevation-%
-100	1.4	1.4	0	0.0
-80	1.4	1.7	40	0.0
-60	1.4	2.0	80*	0.0
-40	1.4	2.2	120	1.0
-20	1.4	2.9	160	1.0
PC	1.4	3.9	200	1.0
+20	0.9	5.2	240**	2.4
+40	0.9	6.2	280	3.8
+60	1.2	6.0	320	3.9
+80	1.4	5.7	360	4.2
+100	1.7	5.5	400	4.6
+120	2.0	5.5	440	4.6
+140	1.7	5.1	480	4.3
+160	1.2	5.0		
+180	1.1	5.8		
+200	1.4	5.8		

*TS is at 70 ft (21.3 m)

**PC is at 220 ft (67.1 m)

1 ft = 0.305 m

Speed data were collected using a two-channel chart recorder equipped with a manual remote event marker. The chart recorder was located in the back seat of the experimental vehicle and was operated by the driver, who noted the time* at which the rear tires of the subject vehicle crossed each of the larger interval markers. Using times between events, speed data could be calculated for each of the three intervals. All data were collected on dry roads, during daylight hours.

Sample Description

For each of the selected curves, data were collected for three specified vehicle types:

1) passenger cars
2) full size school buses
3) tractor-trailers.

It was originally intended to collect data for 30 vehicles of each type on each curve, or 270 vehicle paths. Because of time constraints and the relative infrequency of school bus traffic (and tractor-trailer traffic on the 8° curve), smaller samples were obtained. Sample size was also reduced due to the disqualification of certain vehicles as not being in a free flow condition. Film quality, including difficulty of obtaining required measurements was also responsible for the reduction of sample size. Where data for more than 30 vehicles were collected, the sample was reduced to 30 vehicles based upon the quality of the data. The following table presents the sample sizes for each of the curves in terms of vehicle type.

*Since the driver was able to see the subject vehicle approaching each mark, it was estimated that error due to human reaction time would be minimal (i.e., approximately .1 second).

Table 17.

OBSERVATIONAL SAMPLE

Vehicle Type	38° Curve	8° Curve	31° Curve
Automobile	30	30	30
School Bus	30	13	14
Tractor-Trailer	30	20	30
TOTAL	90	63	74

Data Reduction

Measurements of lateral displacements were taken from projections of the film negatives. For this purpose, a Recordak MPE-1 film reader was used. These readers are especially designed for viewing enlarged images of 35 mm film on a built-in reflection type screen located at desk level.

For each of the pavement markings, the frame in which the right rear tire of the subject vehicle was closest (longitudinally) to the marking was used. On each picture, two measurements were taken: (1) the lateral displacement of the right rear tire from the right road edge, and (2) the width of the road along the same straight line. The pavement marking was used as a guide to ensure that the measurements were taken on a line which was close of perpendicular to the road edge. The rate of exposure was such that for the majority of measurements taken, the vehicle was within approximately six inches on either side of the pavement marking. It was necessary to take the road width measurement in each picture to determine the scale factor since the distance of the camera (in following vehicle) from the subject vehicle varied according to the following distance of the experimental vehicle. It is estimated that the projected images allowed the measurement of lateral distance to within a maximum error of .25 feet (76.2 mm).

Measurements of time between event marks on the chart recording were determined from the known rate of paper movement for calculation of subject vehicle speeds. It is estimated that speed data are accurate within approximately $\pm$ 1 mph (1.6 km/h).

APPENDIX B

HVOSM MODIFICATIONS

As the HVOSM, in its previous form, was able to directly model only four tires on a vehicle, minor modifications were required to the tire radial and side force calculations so that single tire data could be applied to the case of dual rear tires. Given the tire data for a single tire (K_T,* the radial spring rate; A_0, A_1, A_2, A_3, A_4, the coefficients describing the side force resulting from slip and camber angles as a function of tire load normal to the ground), the modified tire force computational procedure can be described as follows.

1. Given the position of the wheel center relative to the ground and the undeformed tire radius, the deformed or rolling radius, h_i, can be computed in the same manner employed previously in the HVOSM.

2. Given h_i, the total radial force from the set of dual tires can be computed (assuming that the total dual tire stiffness can be lumped at a single location, i.e., along a single line of action) from:

$$F_{Ri} = 2 K_T h_i .$$

3. The total tire force normal to the ground can then be calculated as a function of the total radial force (F_{Ri}), the inclination angle (ϕ_{CGi}) and the previous total side force (F_{Si}) in a manner identical to that previously employed.

$$F'_{Ri} = \text{function } (F_{Ri}, \phi_{CGi}, F_{Si}).$$

---

*The notation used here is consistent with that employed in the HVOSM Documentation. The reader is referred to Reference 1.

4. The non-dimensional slip angle variable, $\bar{\beta}_i$, is then computed using one-half the total normal force to the ground in the manner previously employed:

$$\bar{\beta}_i = \text{function (slip angle, } \phi_{CGi}, \frac{F'_{Ri}}{2}).$$

5. Using this $\bar{\beta}_i$, a side force, f_{si} is calculated. This side force is that resulting from one tire of the dual set given the implicit assumption that each tire is loaded the same and experiencing the same slip angle.

$$f_{si} = \text{function } (\bar{\beta}_i).$$

6. The total side force produced by the set of dual tires is then computed as being twice the value calculated in step 5.

$$F_{si} = 2\, f_{si}.$$

This method of simulating dual tires allows input of individual tire parameters but calculates the total side force based on the assumptions that:

1. The radial force and tractive force for a set of duals is equally split between the two tires.

2. The slip angle is identical for each tire of the dual set.

3. The resultant forces acting on each of a set of dual tires can be replaced by a single set of forces acting at a location such that moment compatibility is maintained.

With regard to this third assumption, it is important to chose an effective track for the two sets of dual tires such that the roll moment on the rear axle is unchanged. This is accomplished with the following equation:

$$T_E^2 = \frac{1}{2} (T_O^2 + T_I^2)$$

where

T_E = the effective track of a dual tired axle

T_O = the track of the outside tires of the dual set

T_I = the track of the inside tires of the dual set.

Note that this equation achieves compatibility of the roll moment due to tire radial forces alone. Compatibility with consideration of tire side forces cannot be stated explicitly due to the highly non-linear relationships involved in computation of these side forces.

APPENDIX C

SIMULATED VEHICLE DATA SUMMARY

INPUT PARAMETER	COMPACT (1974 FORD PINTO)	FULL SIZE (1971 AMC AMBASSADOR)	SCHOOL BUS	UNITS
M_S	6.687	8.21	50.679	lb-sec^2/in
M_{UF}	0.381	0.541	4.51	"
M_{UR}	0.567	0.889	5.37	"
I_X	3920.	3960.	74310.	lb-sec^2-in
I_Y	14040.	20350.	1022680.	"
I_Z	16440.	29250.	1019490.	"
I_{XZ}	0.0	0.0	0.0	"
I_F	-	-	3748.	"
I_R	172.	600.	4458.	"
a	43.7	49.2	150.3	in
b	50.9	72.2	94.7	"
T_F	55.0	60.0	80.0	"
T_R	55.8	60.0	72.8	"
ρ_F	-	-	0.0	"
ρ	0.0	0.0	0.0	"
T_{SF}	-	-	29.00	"
T_S	42.2	33.8	37.0	"
R_F	11700.	306000.	167000.	lb-in/rad
R_R	30900.	0.0	161000.	"
K_{RS}	-0.095	-0.151	0.0	deg/deg
Z'_{CO}	-20.28	-24.7	-48.4	in

*The reader is referred to Reference 1 for a description of the HVOSM input parameters.

SIMULATED VEHICLE DATA SUMMARY (continued)

INPUT PARAMETER	COMPACT (1974 FORD PINTO)	FULL SIZE (1971 AMC AMBASSADOR)	SCHOOL BUS	UNITS
K_F	110.0	92.0	550.0	lb/in
K_{FC}	1200.0	220.8	550.0	"
K'_{FC}	283.0	0.0	0.0	lb/in^3
K_{FE}	825.0	220.8	550.	lb/in
K'_{FE}	313.0	0.0	0.0	lb/in^3
Ω_{FC}	-3.37	-4.4	-1.0	in
Ω_{FE}	3.63	1.4	4.25	in
C_F	2.0	3.2	9.5	lb sec/in
C'_F	36.0	70.	200.0	lb
λ_F	0.8	0.8	0.8	-
K_R	107.0	92.0	1100.0	lb/in
K_{RC}	210.0	248.4	1100.0	"
K'_{RC}	283.0	0.0	0.0	lb/in^3
K_{RE}	825.0	248.4	1100.0	lb/in
K'_{RE}	313.0	0.0	0.0	lb/in^3
Ω_{RC}	-3.51	-2.5	-1.0	in
Ω_{RE}	3.26	1.75	4.25	in
C_R	2.0	5.0	19.0	lb-sec/in
C'_R	50.0	20.0	400.0	lb
λ_R	0.8	0.8	0.8	-

SIMULATED VEHICLE DATA SUMMARY (continued)

INPUT PARAMETER	COMPACT (1974 FORD PINTO)	FULL SIZE (1971 AMC AMBASSADOR)	SCHOOL BUS	UNITS
K_T	1270.	1330.	5500.	lb/in
σ_T	6.0	6.0	8.0	in
λ_T	10.0	10.0	10.0	
A_0	1721.5	2701.0	8129.29	
A_1	9.63	10.1	9.8404	
A_2	2146.9	2533.0	15418.7	
A_3	2.691	1.30	1.4406	
A_4	2365.6	4591.0	21646.6	
Ω_T	1.0	1.0	1.0	
R_W	11.72	14.0	20.0	in

FRONT WHEEL CAMBER VS. SUSPENSION DEFLECTION

SUSPENSION DEFLECTION (IN.)	CAMBER ANGLE (DEG) COMPACT (1974 PINTO)	FULL SIZE (1971 AMBASSADOR)
-4	-4.7	0.31
-3	-3.1	-0.3
-2	-1.8	-0.64
-1	-0.7	-0.55
0	0.0	0.0
1	0.4	0.98
2	0.6	1.75
3	0.8	2.32
4	0.82	

APPENDIX D

SPIRAL DEVELOPMENT

The curvature, K, of a line is defined as:

$$K = \left(\frac{d\alpha}{ds}\right) = f(s)$$

where α is the angle of a tangent to the curve and s is the arc length. If f(s) is continuous and greater than zero for $0 \leq s \leq b$ then

$$\alpha(s) = \int_0^s f(s)\, ds + c_1$$

Also, $ds^2 = dx^2 + dy^2$, or

$$\left(\frac{dx}{ds}\right)^2 + \left(\frac{dy}{ds}\right)^2 = 1 \text{ and } \frac{dy}{dx} = \tan \alpha.$$

And, $\frac{dx}{ds} = \cos \alpha \quad \frac{dy}{ds} = \sin \alpha.$

Therefore x and y can be determined as functions of s:

$$x(s) = \int_0^s \cos \alpha \, ds + c_2$$

$$y(s) = \int_0^s \sin \alpha \, ds + c_3$$

If it is assumed that the curvature varies as a linear function of s as:

$$K = as = f(s)$$

then

$$\alpha = \int_0^s as\ ds + c_1 = \frac{as^2}{2} + c_1$$

and

$$x = \int_0^s \cos\left(\frac{as^2}{2} + c_1\right) ds + c_2$$

$$y = \int_0^s \sin\left(\frac{as^2}{2} + c_1\right) ds + c_3$$

Applying the initial conditions:

$$\alpha = \alpha_0 \ @\ s = 0$$

$$x = x_0 \ @\ s = 0$$

$$y = y_0 \ @\ s = 0$$

the position of a point on the curve is obtained as:

$$x = \int_0^s \cos\left(\frac{as^2}{2} + \alpha_0\right) ds + x_0$$

$$y = \int_0^s \cos\left(\frac{as^2}{2} + \alpha_0\right) ds + y_0$$

If it assumed that the speed, v, along the curve is constant then the acceleration is normal to the curve and of magnitude:

$$A = \frac{v^2}{r} = v^2 K$$

then $$\frac{dA}{dt} = v^2 \frac{dK}{dt} .$$

But, $K = as$ and $\frac{dK}{dt} = a\frac{ds}{dt} = av$. Consequently, $\frac{dA}{dt} = av^3 = C$ and $a = \frac{C}{v^3}$. Finally, $K = \frac{C}{v^3} s$.

☆ U. S. GOVERNMENT PRINTING OFFICE : 1980—328-802/6558

FEDERALLY COORDINATED PROGRAM (FCP) OF HIGHWAY RESEARCH AND DEVELOPMENT

The Offices of Research and Development (R&D) of the Federal Highway Administration (FHWA) are responsible for a broad program of staff and contract research and development and a Federal-aid program, conducted by or through the State highway transportation agencies, that includes the Highway Planning and Research (HP&R) program and the National Cooperative Highway Research Program (NCHRP) managed by the Transportation Research Board. The FCP is a carefully selected group of projects that uses research and development resources to obtain timely solutions to urgent national highway engineering problems.*

The diagonal double stripe on the cover of this report represents a highway and is color-coded to identify the FCP category that the report falls under. A red stripe is used for category 1, dark blue for category 2, light blue for category 3, brown for category 4, gray for category 5, green for categories 6 and 7, and an orange stripe identifies category 0.

FCP Category Descriptions

1. Improved Highway Design and Operation for Safety

Safety R&D addresses problems associated with the responsibilities of the FHWA under the Highway Safety Act and includes investigation of appropriate design standards, roadside hardware, signing, and physical and scientific data for the formulation of improved safety regulations.

2. Reduction of Traffic Congestion, and Improved Operational Efficiency

Traffic R&D is concerned with increasing the operational efficiency of existing highways by advancing technology, by improving designs for existing as well as new facilities, and by balancing the demand-capacity relationship through traffic management techniques such as bus and carpool preferential treatment, motorist information, and rerouting of traffic.

3. Environmental Considerations in Highway Design, Location, Construction, and Operation

Environmental R&D is directed toward identifying and evaluating highway elements that affect the quality of the human environment. The goals are reduction of adverse highway and traffic impacts, and protection and enhancement of the environment.

4. Improved Materials Utilization and Durability

Materials R&D is concerned with expanding the knowledge and technology of materials properties, using available natural materials, improving structural foundation materials, recycling highway materials, converting industrial wastes into useful highway products, developing extender or substitute materials for those in short supply, and developing more rapid and reliable testing procedures. The goals are lower highway construction costs and extended maintenance-free operation.

5. Improved Design to Reduce Costs, Extend Life Expectancy, and Insure Structural Safety

Structural R&D is concerned with furthering the latest technological advances in structural and hydraulic designs, fabrication processes, and construction techniques to provide safe, efficient highways at reasonable costs.

6. Improved Technology for Highway Construction

This category is concerned with the research, development, and implementation of highway construction technology to increase productivity, reduce energy consumption, conserve dwindling resources, and reduce costs while improving the quality and methods of construction.

7. Improved Technology for Highway Maintenance

This category addresses problems in preserving the Nation's highways and includes activities in physical maintenance, traffic services, management, and equipment. The goal is to maximize operational efficiency and safety to the traveling public while conserving resources.

0. Other New Studies

This category, not included in the seven-volume official statement of the FCP, is concerned with HP&R and NCHRP studies not specifically related to FCP projects. These studies involve R&D support of other FHWA program office research.

* The complete seven-volume official statement of the FCP is available from the National Technical Information Service, Springfield, Va. 22161. Single copies of the introductory volume are available without charge from Program Analysis (HRD-3), Offices of Research and Development, Federal Highway Administration, Washington, D.C. 20590.